

PaddleOCR-VL-1.5: Towards a Multi-Task 0.9B VLM for Robust In-the-Wild Document Parsing

Cheng Cui, Ting Sun, Suyin Liang, Tingquan Gao, Zelun Zhang, Jiaxuan Liu, Xueqing Wang, Changda Zhou, Hongen Liu, Manhui Lin, Yue Zhang, Yubo Zhang, Yi Liu, Dianhai Yu, Yanjun Ma

PaddlePaddle Team, Baidu Inc.
paddleocr@baidu.com

Official Website: <https://www.paddleocr.com>

Source Code: <https://github.com/PaddlePaddle/PaddleOCR>

Models: <https://huggingface.co/PaddlePaddle>

Abstract

We introduce PaddleOCR-VL-1.5, an upgraded model achieving a new state-of-the-art (SOTA) accuracy of 94.5% on OmniDocBench v1.5. To rigorously evaluate robustness against real-world physical distortions—including scanning, skew, warping, screen-photography, and illumination—we propose the Real5-OmniDocBench benchmark. Experimental results demonstrate that this enhanced model attains SOTA performance on the newly curated benchmark. Furthermore, we extend the model’s capabilities by incorporating seal recognition and text spotting tasks, while remaining a 0.9B ultra-compact VLM with high efficiency.

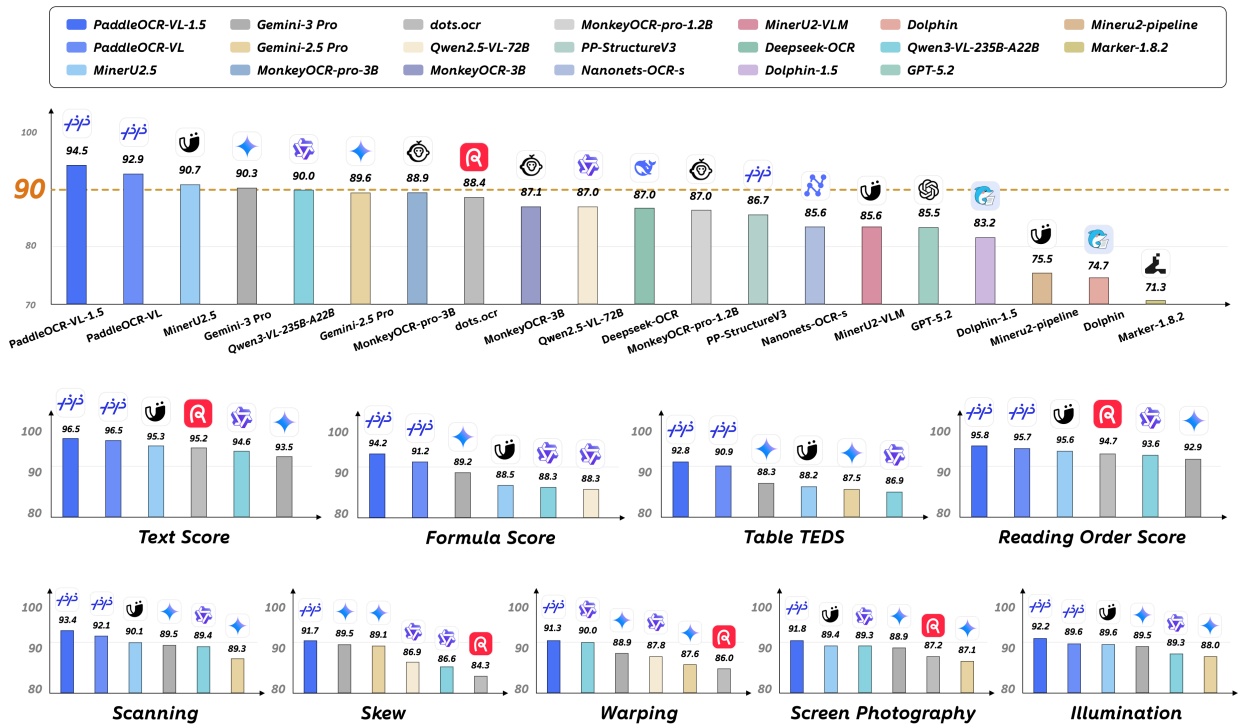


Figure 1 | Performance of PaddleOCR-VL-1.5 on OmniDocBench v1.5 and Real5-OmniDocBench.

Contents

- 1 Introduction** **3**
- 2 PaddleOCR-VL-1.5** **4**
 - 2.1 Architecture 4
 - 2.2 Training Recipe 6
- 3 Dataset** **9**
 - 3.1 Layout Analysis 9
 - 3.2 PaddleOCR-VL-1.5-0.9B 9
- 4 Evaluation** **11**
 - 4.1 Document Parsing 11
 - 4.2 New Capabilities 13
 - 4.3 Inference Performance 14
- 5 Conclusion** **15**
- A Comparison of PaddleOCR-VL-1.5 and 1.0 Models** **19**
- B Details of the Real5-OmniDocBench Benchmark** **20**
- C Supported Languages** **23**
- D Inference Performance on Different Hardware Configurations** **24**
- E Real-world Samples** **25**
 - E.1 Real-word Document Parsing 26
 - E.2 Layout Analysis 31
 - E.3 Text Recognition 36
 - E.4 Table Recognition 39
 - E.5 Formula Recognition 42
 - E.6 Seal Recognition 43
 - E.7 Text Spotting 46

1. Introduction

As the primary repository of human knowledge, documents are growing exponentially in both volume and complexity, establishing document parsing as a pivotal technology in the era of artificial intelligence. The ultimate objective of document parsing [1, 2, 3, 4] extends beyond mere text recognition; it aims to reconstruct the deep structural and semantic layout of a document. By meticulously distinguishing text blocks, decoding complex formulas and tables, and deducing the logical reading order, advanced parsing lays the groundwork for Large Language Models (LLMs) [5, 6, 7]. Crucially, this capability empowers Retrieval-Augmented Generation (RAG) systems [8] to ingest high-fidelity knowledge, thereby enhancing their reliability in downstream applications.

The field has witnessed a surge of innovation following October 2025, with several significant document parsing solutions emerging to push the boundaries of document intelligence. Notably, PaddleOCR-VL [9] established a high performance baseline, surpassing contemporary SOTA metrics with only 0.9 billion parameters and demonstrating strong multi-scenario generalization. Concurrently, DeepSeek-OCR [10] leverages an optical 2D mapping methodology to enable high-ratio vision-to-text compression, offering robust end-to-end parsing capabilities. MonkeyOCR v1.5 [11] further enhances the three-stage parsing framework, while HunyuanOCR [12] extends expert OCR capabilities through a unified architecture supporting translation and extraction.

Despite these advancements, a critical gap remains: most existing models are primarily optimized for "digital-born" or cleanly scanned documents. Real-world scenarios involving extreme physical distortions—such as aggressive skewing, non-rigid warping of pages, screen-capture moiré patterns, and erratic lighting—remain significant hurdles that even state-of-the-art solutions have yet to fully overcome.

To bridge this gap, we present PaddleOCR-VL-1.5, a high-performance, resource-efficient document parsing solution that significantly enhances both general precision and real-world robustness. Building upon the proven 0.9B ultra-compact architecture, PaddleOCR-VL-1.5 introduces several critical advancements:

- Firstly, we upgrade the layout engine to PP-DocLayoutV3. Unlike previous Layout Analysis methods (e.g., Dolphin [3], MinerU2.5 [2], or even PP-DocLayoutV2 [13]), PP-DocLayoutV3 is specifically engineered to handle non-planar document images. It can directly predict multi-point bounding boxes for layout elements—as opposed to standard two-point boxes—and determine logical reading orders for skewed and warped surfaces within a single forward pass, significantly reducing cascading errors.
- Secondly, we expand the model’s core capabilities. While maintaining the efficient NaViT-style dynamic resolution encoder and the ERNIE-4.5-0.3B [5] language backbone, we have integrated new tasks including seal recognition and text spotting. Systematic optimizations in text, table, and formula recognition have further propelled the model to a new performance milestone.
- Thirdly, we construct Real5-OmniDocBench to evaluate in-the-wild robustness. Recognizing the lack of benchmarks for physical distortions, we curated this dataset based on OmniDocBench v1.5 [14]. It comprises five distinct scenarios: scanning, warping, screen photography, illumination, and skew. By maintaining a strict one-to-one correspondence with the original ground-truth annotations, Real5-OmniDocBench serves as a rigorous benchmark for assessing model resilience in practical applications.

Comprehensive benchmarking confirms that PaddleOCR-VL-1.5 establishes a new state-

of-the-art (SOTA) standard. On the OmniDocBench v1.5 benchmark, our model achieves a breakthrough accuracy of 94.5%, maintaining its position as the official top-ranked solution. More importantly, on the newly curated Real5-OmniDocBench, the model sets a new record with an overall accuracy of 92.05%. Despite its compact 0.9B scale, it significantly outperforms massive general VLMs, such as Qwen3-VL-235B [6] and Gemini-3 Pro [15], highlighting its exceptional parameter efficiency. Furthermore, our model expands its capabilities to text spotting and seal recognition, attaining leading performance across diverse and challenging benchmarks. These results collectively validate its superior robustness and generalization in complex, real-world scenarios. Appendix A details the specific upgrades and changes in PaddleOCR-VL-1.5 compared to its predecessor.

2. PaddleOCR-VL-1.5

2.1. Architecture

PaddleOCR-VL-1.5 introduces an enhanced framework capable of handling both Document Parsing and Text Spotting, as depicted in Figure 2.

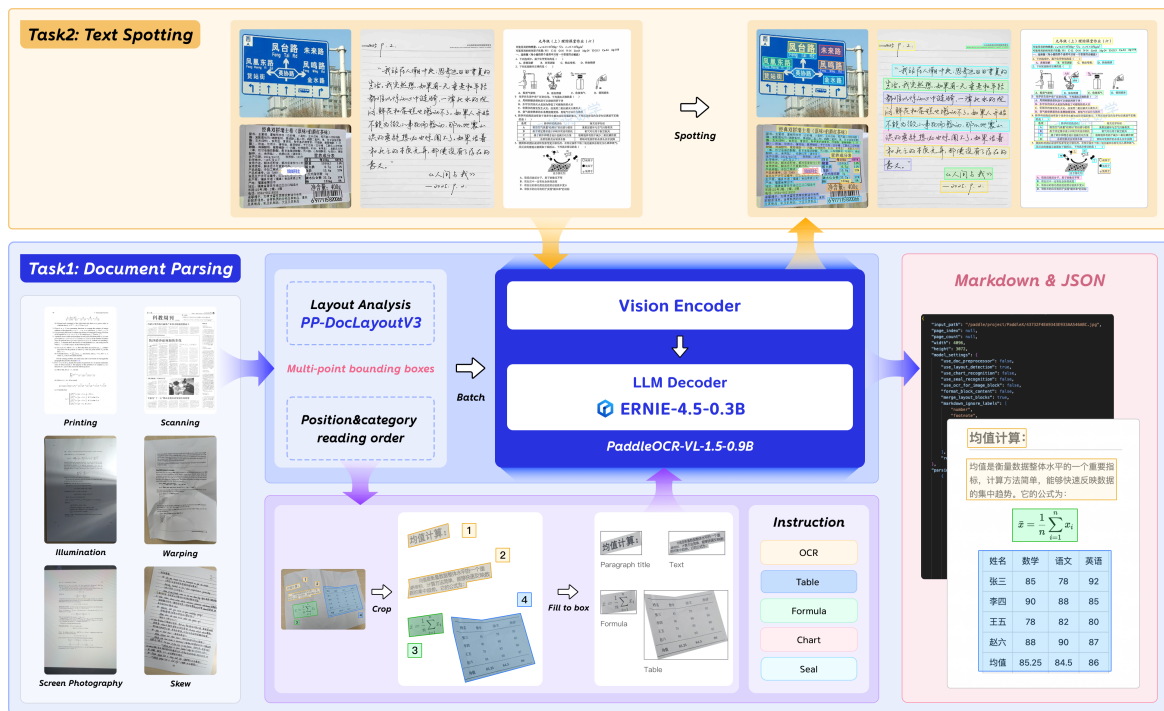


Figure 2 | The overview of PaddleOCR-VL-1.5.

For the Document Parsing task, PaddleOCR-VL-1.5 adopts a robust two-stage framework. In the initial stage, PP-DocLayoutV3 performs sophisticated layout analysis. Beyond standard axis-aligned detection, it is specifically optimized for real-world complexity by employing multi-point localization (e.g., quadrilaterals or polygons). This allows for the precise boundary anchoring of semantic regions even under severe perspective tilt or physical curvature, while simultaneously establishing the logical reading order. In the second stage, the PaddleOCR-VL-1.5-0.9B model takes these geometrically-rectified or localized regions as input to perform

high-fidelity recognition across diverse modalities, including text, complex tables, mathematical formulas, charts and seals. To conclude the pipeline, a lightweight post-processing engine orchestrates these outputs into structured formats such as Markdown and JSON, while providing advanced capabilities such as cross-page table merging and heading hierarchy refinement.

For the Spotting task, the framework simplifies its workflow by directly utilizing the PaddleOCR-VL-1.5-0.9B model for end-to-end text detection and recognition. This approach enables end-to-end text detection and recognition across a wide spectrum of domains—ranging from standard documents, identification cards, and ancient manuscripts to unconstrained scenarios like advertising posters, dialogue screenshots, signboards, and multilingual texts.

2.1.1. PP-DocLayoutV3: Unified Layout Analysis

To address the challenges of complex physical distortions—including skew, warping, and illumination—and to overcome the high latency inherent in autoregressive Vision-Language Models (VLMs), we introduce PP-DocLayoutV3. This version represents a significant architectural evolution from its predecessor by transitioning from standard rectangular detection to a robust instance segmentation framework, while simultaneously integrating reading order prediction into a unified, end-to-end Transformer architecture.

Building upon the high-efficiency RT-DETR object detector [16], PP-DocLayoutV3 adopts a mask-based detection head. This allows the model to predict precise, pixel-accurate masks for layout elements rather than simple bounding boxes. Such a capability is critical for isolating document components in non-ideal scenarios, such as skewed or warped pages, where traditional axis-aligned boxes frequently overlap or capture excessive background noise.

Unlike the decoupled pointer network employed in PP-DocLayoutV2 [9], PP-DocLayoutV3 integrates Reading Order Prediction directly into the Transformer decoder layers. By merging detection, segmentation, and ordering into a single vision-centric model, PP-DocLayoutV3 eliminates the need for redundant post-processing and separate feature extraction steps.

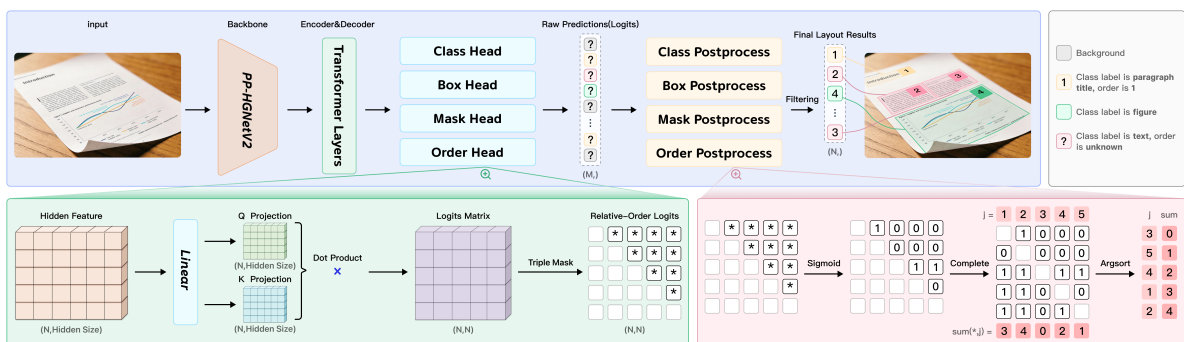


Figure 3 | The unified architecture of PP-DocLayoutV3, featuring parallel heads for instance segmentation and relational reading order prediction.

The core architectural innovation of PP-DocLayoutV3 is the integration of Reading Order Prediction directly into the Transformer decoder. Specifically, our model extends the RT-DETR framework to simultaneously optimize geometric localization and logical sequencing. Following the query-based paradigm, the decoder iteratively refines N object queries $Q = \{q_i\}_{i=1}^N \in \mathbb{R}^{N \times d}$. The reading order is then derived from the refined query embeddings of the final decoder layer through a Global Pointer Mechanism.

We project the refined queries into a shared relational space to compute the pairwise precedence score $S_{i,j}$:

$$S_{i,j} = \frac{f(q_i, q_j) - f(q_j, q_i)}{\sqrt{d_h}}, \quad \text{where } f(q_i, q_j) = (W_q q_i)^\top (W_k q_j) \quad (1)$$

where $W_q, W_k \in \mathbb{R}^{d \times d_h}$ are learnable projection matrices and d_h denotes the hidden dimension. The resulting relation matrix $S \in \mathbb{R}^{N \times N}$ is constrained to be anti-symmetric such that $S_{i,j} = -S_{j,i}$, where $S_{i,j} > 0$ implies element i precedes element j .

During inference, to derive a globally consistent sequence from these pairwise relations, we implement a Voting-based Ranking strategy. We first apply the sigmoid function $\sigma(\cdot)$ to the relation matrix S and mask the diagonal elements. The absolute precedence votes V_j for each element j is computed by aggregating the probabilities of other elements preceding it:

$$V_j = \sum_{i=1, i \neq j}^N \sigma(S_{i,j}). \quad (2)$$

The final reading order is determined by sorting the elements in ascending order of their total votes V_j . This joint optimization ensures that the logical sequence is highly sensitive to the refined object features, leading to superior performance on complex, multi-column, and non-standard document layouts.

By merging detection, segmentation, and ordering into a single vision-centric model, PP-DocLayoutV3 eliminates the need for redundant post-processing and separate feature extraction. The model produces the complete document structure in a single forward pass, where the multi-head system concurrently outputs classification labels, bounding box coordinates, pixel-accurate segments, and the logical reading sequence.

2.1.2. PaddleOCR-VL-1.5-0.9B: Element-level Recognition and Text Spotting

The PaddleOCR-VL-1.5-0.9B inherits the lightweight architecture of PaddleOCR-VL-0.9B [9], integrating a Native Resolution Visual Encoder [17], an Adaptive MLP Connector, and the Lightweight ERNIE-4.5-0.3B Language Model [5]. In this update, the model’s capabilities have been expanded to include Seal Recognition and Text Spotting. Consequently, the model now supports a comprehensive set of six core tasks: OCR, Formula Recognition, Table Recognition, Chart Recognition, Seal Recognition, and Text Spotting.

Compared to its predecessor, PaddleOCR-VL-1.5-0.9B demonstrates significant enhancements in recognition accuracy for complex tables and mathematical formulas. Furthermore, the model incorporates finer-grained optimizations for rare characters, ancient Chinese texts, multilingual tables, and text decorations such as underlines and emphasis marks.

2.2. Training Recipe

The following sections introduce the training details of these two modules: PP-DocLayoutV3 for layout analysis and PaddleOCR-VL-1.5-0.9B for element recognition and text spotting.

2.2.1. Layout Analysis

The training of PP-DocLayoutV3 evolves from the two-stage decoupled process used in PP-DocLayoutV2 [9] to a more sophisticated end-to-end joint optimization strategy. This approach allows the detection, instance segmentation, and reading order modules to share a unified feature representation, leading to better alignment between spatial localization and logical sequencing.

The model is initialized with the pre-trained weights of PP-DocLayout_plus-L [13], we scaled our training corpus to over 38k high-quality document samples. Each sample underwent rigorous manual annotation to provide ground truth, include the coordinates, categorical label and absolute reading order for every layout elements.

To achieve the environmental robustness, we designed a specialized Distortion-Aware Data Augmentation pipeline. Unlike standard augmentations, this pipeline specifically simulates complex physical deformations found in real-world mobile photography.

We utilize the AdamW optimizer with a weight decay of 0.0001. The learning rate is set to a constant 2×10^{-4} to ensure stable convergence of the integrated Global Pointer and Mask heads. The model is trained for 150 epochs with a total batch size of 32.

In contrast to the previous version, all components—including the RT-DETR backbone and the integrated reading order transformer—are trained simultaneously. This end-to-end supervision ensures that the learned queries in the Transformer decoder capture both the geometric boundaries and the topological relationships of the document elements.

2.2.2. Element-level Recognition and Text Spotting

Building upon the architecture described in Section 2.1.2, PaddleOCR-VL-1.5-0.9B introduces a progressive training paradigm using PaddleFormers [18], which is a high-performance training toolkit for LLMs and VLMs built on the PaddlePaddle framework [19]. While we retain the effective post-adaptation strategy and initialization settings from our previous version, the training methodology has been significantly upgraded to enhance data scale, task diversity, and model robustness. The overview of the three stages is presented in Table 1.

Settings	Pre-training	Post-training
Training Samples	46M	5.6M
Max Resolution	$1280 \times 28 \times 28$	$1280 \times 28 \times 28$
Sequence length	16384	16384
Trainable components	All	All
Batch sizes	128	128
Data Augmentation	Yes	Yes
Maximum LR	5×10^{-5}	8×10^{-6}
Epoch	1	1

Table 1 | Training settings for PaddleOCR-VL-1.5-0.9B.

Pre-training: Enhanced Vision-Language Alignment. While the fundamental objective remains aligning visual features with textual semantics, this stage undergoes a substantial data upgrade compared to PaddleOCR-VL-0.9B [9], scaling the pre-training dataset from 29 million to 46 million image-text pairs. This expansion represents a qualitative leap in data distribution rather than a mere quantitative increase. Specifically, to enhance the generalization of the visual backbone and support the newly introduced capabilities, we incorporate a broader spectrum of multilingual documents and complex real-world scenarios. Furthermore, we intentionally inject

large-scale pre-training data related to seal recognition and text spotting during this alignment phase. Specifically, the maximum resolution for the spotting task is increased to $2048 \times 28 \times 28$ pixels, enabling the model to achieve more precise localization and recognition of text. By introducing these task-specific priors early in the training pipeline, the model establishes a robust foundation capable of capturing intricate visual patterns and effectively supporting the fine-grained localization and recognition tasks required in subsequent stages.

Post-training: Instruction Fine-tuning with New Capabilities. In this stage, we inherit the four fundamental instruction tasks from PaddleOCR-VL-0.9B—**OCR, Table, Formula, and Chart Recognition**—ensuring backward compatibility and high performance on standard document elements. The key innovation in PaddleOCR-VL-1.5-0.9B lies in the addition of two specialized tasks:

1. **Seal Recognition:** We introduce a specific instruction to handle official seals and stamps, addressing challenges such as curved text, blur images and background interference.
2. **Text Spotting (Grounded OCR):** Unlike standard OCR, which solely outputs textual content, the text spotting task requires the model to simultaneously predict the text and its precise spatial location following the natural reading order. To accommodate complex layouts found in real-world scenarios (e.g., rotated text, common scene, or dense forms), we adopt a **4-point quadrilateral representation** rather than the traditional 2-point bounding box. The 4-point format defines a text region using four vertices: Top-Left (TL), Top-Right (TR), Bottom-Right (BR), and Bottom-Left (BL). This formulation provides superior flexibility in localizing inclined and irregular text shapes that a standard axis-aligned rectangle cannot tightly enclose. Formally, for a given text instance, the target sequence is constructed by appending eight location tokens to the text tokens:

$$Y = \text{Text} \oplus \langle \text{LOC}_{x_{TL}} \rangle \langle \text{LOC}_{y_{TL}} \rangle \dots \langle \text{LOC}_{y_{BL}} \rangle \quad (3)$$

Here, we introduce a set of tokens $\{\langle \text{LOC}_0 \rangle, \dots, \langle \text{LOC}_{1000} \rangle\}$ to the model’s vocabulary to represent normalized coordinates. Unlike treating coordinates as plain numerical text, these dedicated special tokens allow the model to learn specific embeddings for spatial information and prevent tokenization fragmentation.

For example, a recognized instance of the word "DREAM" is represented as:

DREAM $\langle \text{LOC}_{253} \rangle \langle \text{LOC}_{286} \rangle \langle \text{LOC}_{346} \rangle \langle \text{LOC}_{298} \rangle \langle \text{LOC}_{345} \rangle \langle \text{LOC}_{339} \rangle \langle \text{LOC}_{252} \rangle \langle \text{LOC}_{330} \rangle$

This unified representation enables the model to perform end-to-end recognition and fine-grained localization within a single generation pass.

To enhance generalization and unify diverse label styles, we introduce a Reinforcement Learning stage leveraging Group Relative Policy Optimization (GRPO) [20]. By executing parallel rollouts and calculating relative advantages within each group, GRPO facilitates robust policy updates and mitigates style inconsistency. This process is supported by a dynamic data screening protocol that prioritizes challenging samples with high reward potential and entropy uncertainty, ensuring the model focuses on non-trivial, high-value learning cases.

3. Dataset

3.1. Layout Analysis

To ensure robust model performance across diverse real-world document scenarios, we curate a in-house dataset for layout analysis. The data sources encompass 38k document images across diverse domains, including Academic papers, Textbooks, Market Analysis, Financial reports, Slides, Newspapers, Supplementary Teaching Materials, Examination Papers, and various Invoices and Receipts. The dataset features meticulous manual annotations across 25 distinct component categories: Paragraph Title, Image, Text, Number, Abstract, Content, Figure Title, Display Formula, Table, Reference, Doc Title, Footnote, Header, Algorithm, Footer, Seal, Chart, Formula Number, Aside Text, Reference Content, Header Image, Footer Image, Inline Formula, Vertical Text, and Vision Footnote. All documents are manually annotated with element-level boundaries and their corresponding reading order, enabling effective training and evaluation for both layout element detection and reading order restoration. This high-quality ground truth ensures that the model can accurately reconstruct both the spatial structure and the logical flow of complex documents.

The data curation process incorporates specific data mining strategies aimed at expanding dataset diversity and identifying hard cases to improve model robustness. This workflow begins with clustering-based sampling applied to an extensive internal data pool, utilizing visual features to ensure a representative distribution and minimize redundancy. Subsequently, a hard-case mining pipeline is executed using PP-DocLayoutV2 [9] for dual-threshold inference. Samples exhibiting a significant discrepancy in detection density between high and low confidence thresholds are categorized as unstable cases. This methodology facilitates the systematic discovery of non-conventional layout structures—including comics, CAD drawings, and high-aspect ratio screenshots—which diverge from standard document formats. These instances are further refined through a human-in-the-loop process. Integrating these diverse scenarios into the dataset broadens the model’s representation of characteristics and enhances its adaptive capacity in complex real-world document domains.

3.2. PaddleOCR-VL-1.5-0.9B

The data construction strategy for PaddleOCR-VL-1.5-0.9B is driven by two core objectives: enhancing model robustness on challenging samples and expanding the breadth of supported capabilities. Consequently, our data preparation pipeline is divided into two distinct parts: (1) **Hard Example Mining** (Section 3.2.1), which focuses on identifying and weighting high-uncertainty samples to refine the model’s decision boundaries; and (2) **New Capability Data Construction** (Section 3.2.2), which involves curating specialized datasets to unlock new skills such as text spotting, seal recognition, and advanced multilingual support.

3.2.1. Data Selection Strategy: Uncertainty-Aware Cluster Sampling

To maximize the efficiency of the instruction fine-tuning stage (Stage 2), we propose a data curation strategy designed to balance visual diversity and sample difficulty. Instead of uniform random sampling, we employ an **Uncertainty-Aware Cluster Sampling (UACS)** mechanism. This approach ensures that the training data covers a wide spectrum of visual scenarios while allocating more training budget to "hard" cases where the model exhibits high uncertainty.

1. Visual Feature Clustering. First, to guarantee the diversity of visual layouts across the six tasks (OCR, Table, Formula, Chart, Seal, and Spotting), we utilize the CLIP [21] visual encoder to

extract high-dimensional semantic embeddings for all candidate images. For each task, we apply K-Means clustering to partition the dataset \mathcal{D} into K distinct visual clusters $\{C_1, C_2, \dots, C_K\}$. This step groups samples with similar visual structures (e.g., solid line tables vs. wireless tables) together.

2. Uncertainty Estimation. For each cluster C_i , we estimate its difficulty by measuring the model’s prediction uncertainty. Specifically, we randomly sample a subset of images from C_i and perform multiple inference passes with stochastic decoding using the pre-trained model from Stage 1. We calculate an uncertainty score S_i based on the divergence of the generated outputs. A higher S_i indicates that the model is inconsistent or unconfident regarding the samples in this cluster.

3. Weighted Sampling Plan. Based on the uncertainty score, we formulate a sampling plan to determine the number of samples N_i to draw from each cluster C_i . Inspired by the principle of hard example mining, we adopt a polynomial weighting scheme to amplify the focus on harder clusters. Specifically, the allocated sample count N_i for cluster C_i is determined by:

$$N_i = \min \left(\left\lfloor \frac{(S_i + \alpha)^\beta}{\sum_{j=1}^K (S_j + \alpha)^\beta} \times N_{\text{total}} \right\rfloor, |C_i| \right) \quad (4)$$

where S_i is the average uncertainty score of cluster C_i , and $|C_i|$ denotes the total number of available samples in that cluster. The parameters α and β are the smoothing and power factors, respectively (set to $\alpha = 1.0, \beta = 2.0$ based on empirical observations). N_{total} represents the total sampling budget. This strategy allows us to dynamically up-sample complex scenarios (e.g., distorted seals, dense tables) while maintaining a representative baseline for simpler cases.

As detailed in the previous section, we employ the Uncertainty-Aware Cluster Sampling (UACS) strategy to select the most effective training samples based on visual clustering and inference variance.

3.2.2. Data Construction for New Capabilities

In addition to data quality control, we expanded the VLM’s capabilities by integrating data spanning a wider array of tasks, languages, and document types. This expansion focuses on these key dimensions: **Spotting, Specialized Text (Seals), OCR Enhancement, and Complex Tables, Formulas, and Chart.**

Spotting: We collected a large-scale and diverse set of images covering a wide range of real-world scenarios, such as financial research reports, tabular documents, handwritten materials, classical texts, and other complex document and natural scene images. During the annotation process, we jointly employed PP-OCRv5 [22] to generate initial recognition results, followed by an IoU-based cross-filtering strategy to eliminate low-quality and inconsistent samples, while for a subset of samples with ambiguous or inaccurate labels, multimodal models including PaddleOCR-VL [9] and Qwen3-VL [6] were further leveraged for label refinement, thereby substantially improving the overall annotation quality and robustness of the dataset.

Seal: We combined synthetic and real-world images of contracts, invoices, and commemorative seals to build a high-quality dataset. Labels were generated using Qwen3-VL [6] and refined through a fine-tuning-based re-labeling process. Challenging cases were manually corrected to ensure final annotation accuracy and robustness.

OCR: We have significantly enhanced the model’s capabilities by refining the dataset’s

precision and enlarging the functional scope. This includes systematically correcting formula representations and line-breaking logic, alongside extending support for education-specific markings like emphasis dots and underlines to capture instructional semantics. Furthermore, the integration of Bengali and China’s Tibetan scripts broadens the model’s linguistic versatility, ensuring robust performance across diverse writing systems and educational contexts.

Formula: Formula dataset incorporates CV-simulated artifacts, such as Gaussian illumination and harmonic moiré, to replicate physical conditions like scanning, warping, screen-capture, and geometric skewing. These samples encompass a wide spectrum of environmental variables, including light fluctuations and complex document distortions encountered in realistic scenarios.

Table: Tables has been expanded to cover an extensive range of scenarios, including financial reports, academic papers, and complex industrial forms. Integration of diverse structures, such as registration and catalog tables. A key focus is placed on the precise recognition of cell-level formulas and multilingual content within dense table environments. These advancements ensure high-fidelity conversion into structured formats, even when handling intricate cell structures and professional notations.

4. Evaluation

To thoroughly assess the effectiveness of PaddleOCR-VL-1.5, we conducted evaluations on the document parsing benchmark OmniDocBench v1.5 and its derived real-world dataset, Real5-OmniDocBench. Furthermore, we expanded the evaluation scope by incorporating text spotting and seal recognition tasks to provide a more comprehensive analysis of the model’s performance in practical and complex scenarios.

4.1. Document Parsing

This section details the evaluation of end-to-end document parsing capabilities using the following two benchmarks, aiming to measure its overall performance in real-world document scenarios.

OmniDocBench v1.5 To comprehensively evaluate the document parsing capabilities, we conducted extensive experiments on the OmniDocBench v1.5 [2] benchmark. It is an expansion of version v1.0, adding 374 new documents for a total of 1,355 document pages. It features a more balanced distribution of data in both Chinese and English, as well as a richer inclusion of formulas and other elements. Compared to version v1.0, the evaluation method has been updated. While text and reading order are still evaluated using Edit Distance, and tables are evaluated using Tree-Edit-Distance-based Similarity (TEDS), formulas are now assessed using the Character Detection Matching (CDM) [23] method. This metric provides a more objective and robust evaluation of the correctness of predicted formulas. The overall metric is a weighted combination of the metrics for text, formulas, and tables.

Table 2 demonstrates that PaddleOCR-VL-1.5 achieves SOTA performance, consistently outperforming existing pipeline tools, general VLMs, and specialized document parsing models across all key metrics. Notably, PaddleOCR-VL-1.5 exhibits a substantial performance leap over its predecessor, PaddleOCR-VL, raising the overall score from 92.86% to a top-ranking 94.50%. Specifically, it achieves increases of 2.99%, 1.87%, and 0.1% in the CDM Score, Table-TEDS, and Reading Order scores, respectively. Furthermore, our model establishes new SOTA results in all sub-tasks, including a reduced Text-Edit distance of 0.035, an improved Formula-CDM

Model Type	Methods	Parameters	Overall \uparrow	Text $^{\text{Edit}}\downarrow$	Formula $^{\text{CDM}}\uparrow$	Table $^{\text{TEDS}}\uparrow$	Table $^{\text{TEDS-S}}\uparrow$	Reading Order $^{\text{Edit}}\downarrow$
Pipeline Tools	Marker-1.8.2 [24]	-	71.30	0.206	76.66	57.88	71.17	0.250
	Mineru2-pipeline [25]	-	75.51	0.209	76.55	70.90	79.11	0.225
	PP-StructureV3 [22]	-	86.73	0.073	85.79	81.68	89.48	0.073
General VLMs	GPT-4o [7]	-	75.02	0.217	79.70	67.07	76.09	0.148
	InternVL3-76B [26]	76B	80.33	0.131	83.42	70.64	77.74	0.113
	InternVL3.5-241B [27]	241B	82.67	0.142	87.23	75.00	81.28	0.125
	GPT-5.2 [28]	-	85.50	0.123	86.11	82.66	87.35	0.099
	Qwen2.5-VL-72B [29]	72B	87.02	0.094	88.27	82.15	86.22	0.102
	Gemini-2.5 Pro [30]	-	88.03	0.075	85.82	85.71	90.29	0.097
	Qwen3-VL-235B-A22B-Instruct [6]	235B	89.15	0.069	88.14	86.21	90.55	0.068
	Gemini-3 Pro [15]	-	90.33	0.065	89.18	88.28	90.29	0.071
Specialized VLMs	Dolphin [3]	0.3B	74.67	0.125	67.85	68.70	77.77	0.124
	OCRFlux-3B [31]	3B	74.82	0.193	68.03	75.75	80.23	0.202
	Mistral OCR [32]	-	78.83	0.164	82.84	70.03	78.04	0.144
	POINTS-Reader [4]	3B	80.98	0.134	79.20	77.13	81.66	0.145
	olmOCR-7B [33]	7B	81.79	0.096	86.04	68.92	74.77	0.121
	Dolphin-1.5 [3]	0.3B	83.21	0.092	80.78	78.06	84.10	0.080
	MinerU2-VLM [25]	0.9B	85.56	0.078	80.95	83.54	87.66	0.086
	Nanonets-OCR-s [34]	3B	85.59	0.093	85.90	80.14	85.57	0.108
	MonkeyOCR-pro-1.2B [1]	1.9B	86.96	0.084	85.02	84.24	89.02	0.130
	Deepseek-OCR [10]	3B	87.01	0.073	83.37	84.97	88.80	0.086
	MonkeyOCR-3B [1]	3.7B	87.13	0.075	87.45	81.39	85.92	0.129
	dots.ocr [35]	3B	88.41	0.048	83.22	86.78	90.62	0.053
	MonkeyOCR-pro-3B [1]	3.7B	88.85	0.075	87.25	86.78	90.63	0.128
	MinerU2.5 [2]	1.2B	90.67	0.047	88.46	88.22	92.38	0.044
	PaddleOCR-VL [9]	0.9B	92.86	0.035	91.22	90.89	94.76	0.043
	PaddleOCR-VL-1.5	0.9B	94.50	0.035	94.21	92.76	95.79	0.042

Table 2 | Comprehensive evaluation on OmniDocBench v1.5. Performance metrics are cited from the official leaderboard [14], except for Gemini-3 Pro, GPT-5.2, Qwen3-VL-235B-A22B-Instruct and our model, which were evaluated independently.

score of 94.21%, and leading scores of 92.76% and 95.79% in Table-TEDS and Table-TEDS-S, respectively. These improvements, particularly in maintaining a high reading ordering score of 0.042, underscore the model’s enhanced precision in text recognition, formula extraction, and complex table structure analysis.

Real5-OmniDocBench Real5-OmniDocBench [36] is a brand-new benchmark oriented toward real-world scenarios, which we constructed based on the OmniDocBench v1.5 dataset. The dataset comprises five distinct scenarios: scanning, warping, screen photography, illumination, and Skew. Apart from the Scanning category, all images were manually acquired via handheld mobile devices to closely simulate real-world conditions. Each subset maintains a one-to-one correspondence with the original OmniDocBench, strictly adhering to its ground-truth annotations and evaluation protocols. Given its empirical and realistic nature, this dataset serves as a rigorous benchmark for assessing the robustness of document parsing models in practical applications. Figure 4 illustrates the visualization of representative samples from the proposed dataset.

As illustrated in Table 3, PaddleOCR-VL-1.5 demonstrates consistent superiority across all evaluated scenarios, setting a new SOTA record with an overall accuracy of 92.05%. Despite its compact 0.9B parameter scale, the model significantly outperforms massive general VLMs, such as Qwen3-VL-235B and Gemini-3 Pro, highlighting its exceptional parameter efficiency for document-centric tasks. Notably, in the highly challenging Skewing category, PaddleOCR-VL-1.5 achieves an accuracy of 91.66%, representing a 14.19% absolute improvement over its predecessor. This substantial performance leap underscores its superior robustness against extreme geometric distortions and validates its reliability for complex document parsing in

unconstrained environments. Detailed comparisons across sub-items including text, formulas, tables, and reading order can be found in Appendix B.

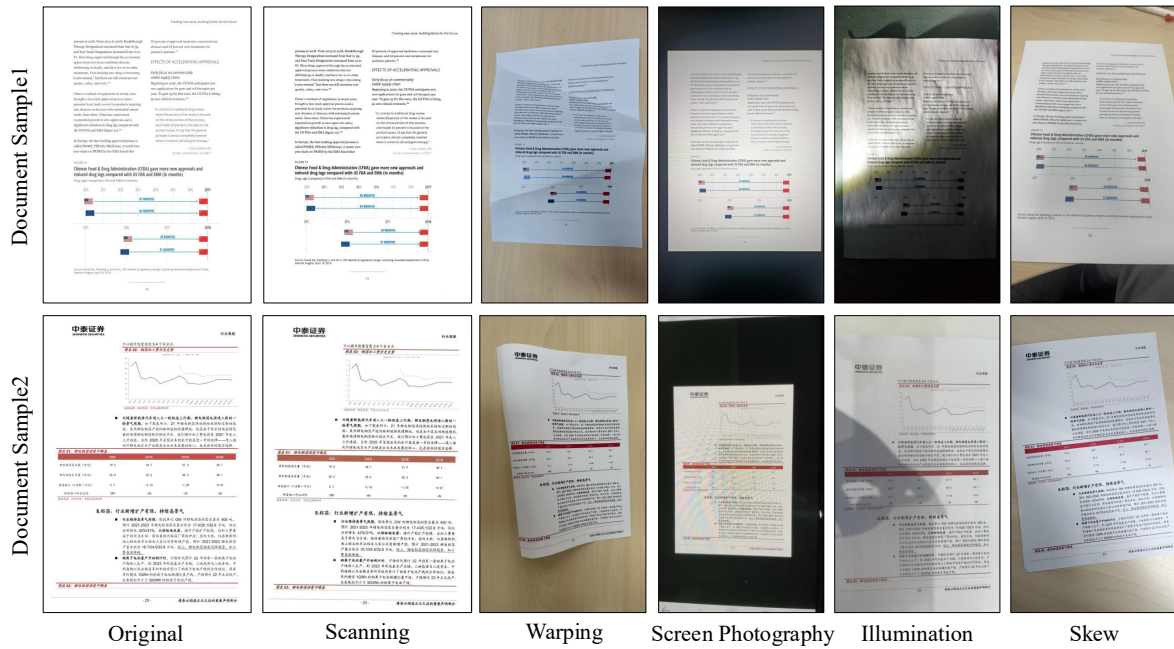


Figure 4 | Samples of Real5-OmniDocBench.

Model Type	Methods	Parameters	Overall↑	Scanning↑	Warping↑	Screen Photography↑	Illumination↑	Skew↑
Pipeline Tools	Maker-1.8.2 [24]	-	60.10	70.27	58.98	63.65	66.31	41.27
	PP-StructureV3 [22]	-	64.45	84.68	59.34	66.89	73.38	37.98
General VLMs	GPT-5.2 [28]	-	78.66	84.43	76.26	76.75	80.88	75.00
	Qwen2.5-VL-72B [29]	72B	86.92	86.19	87.77	86.48	87.25	86.90
	Gemini-2.5 Pro [30]	-	88.21	89.25	87.63	87.11	87.97	89.07
	Qwen3-VL-235B-A22B-Instruct [6]	235B	88.904	89.43	89.99	89.27	89.27	86.56
	Gemini-3 Pro [15]	-	89.24	89.47	88.90	88.86	89.53	89.45
Specialized VLMs	Dolphin-1.5 [3]	0.3B	61.48	83.39	50.50	69.76	75.61	28.16
	Dolphin [3]	0.3B	61.78	72.16	60.35	64.29	67.29	44.83
	Deepseek-OCR [10]	3B	73.99	86.17	67.20	75.31	78.10	63.01
	MinerU2-VLM [25]	0.9B	76.95	83.60	73.73	78.77	80.51	68.16
	MonkeyOCR-pro-1.2B [1]	1.9B	77.15	84.64	76.59	80.24	82.11	62.18
	MonkeyOCR-3B [1]	3.7B	78.29	84.65	77.27	80.71	83.16	65.67
	MonkeyOCR-pro-3B [1]	3.7B	79.49	86.94	78.90	82.44	84.71	64.47
	Nanonets-OCR-s [34]	3B	84.19	85.52	83.56	84.86	85.01	81.98
	PaddleOCR-VL [9]	0.9B	85.54	92.11	85.97	82.54	89.61	77.47
	MinerU2.5 [2]	1.2B	85.61	90.06	83.76	89.41	89.57	75.24
	dots.ocr [35]	3B	86.38	86.87	86.01	87.18	87.57	84.27
	PaddleOCR-VL-1.5	0.9B	92.05	93.43	91.25	91.76	92.16	91.66

Table 3 | Comprehensive evaluation of document parsing on Real5-OmniDocBench, Appendix B provides more detailed metrics of this benchmark.

4.2. New Capabilities

4.2.1. Text Spotting

To thoroughly assess the model’s end-to-end text spotting capability (detection + recognition), we establish a comprehensive OCR benchmark spanning 10 key dimensions. In addition to

standard settings such as common scenes (Common) and multilingual recognition (Japanese), the benchmark is designed to reflect practical deployment challenges by deliberately sampling more difficult cases, including degraded or low-quality images (Blur), highly variable handwriting in both Chinese and English (Handwrite_ch/en), structured and layout-sensitive table content (Table), and culturally significant historical materials such as ancient documents and Traditional Chinese (Ancient). As summarized in Table 4, our model delivers the highest spotting accuracy across all 9 dimensions, consistently outperforming strong baselines and demonstrating robust generalization under diverse visual conditions and text styles. These results indicate that the proposed approach remains reliable not only in regular document scenarios but also in challenging, real-world settings that require precise localization and faithful transcription.

Dataset	Overall	Ancient	Blur	Common	Handwrite_ch	Handwrite_en	Printing_ch	Printing_en	Table	Japanese
HunyuanOCR [12]	0.6290	0.6164	0.6392	0.5222	0.7984	0.7665	0.6213	0.5956	0.4419	0.6593
Rex-Omni [37]	0.6682	0.4251	0.6936	0.6112	0.8147	0.7812	0.6961	0.6088	0.7185	0.6642
PaddleOCR-VL-1.5	0.8621	0.8523	0.8422	0.7713	0.8952	0.9163	0.8669	0.8689	0.8993	0.8461

Table 4 | Comparison of text spotting performance on the in-house benchmark. Overall denotes the average accuracy across all 9 evaluation dimensions.

4.2.2. Seal Recognition

To evaluate the effectiveness of our model in complex seal recognition tasks, we constructed a specialized benchmark comprising 300 high-quality images. This evaluation set covers a diverse range of seal shapes (e.g., circular, oval, and rectangular) and challenging real-world scenarios, such as overlapping text, low-contrast impressions, and distorted backgrounds. We employ the Normalized Edit Distance (NED) as the primary evaluation metric to assess recognition accuracy at the character level.

As illustrated in Table 5, PaddleOCR-VL-1.5 demonstrates a clear advantage in seal recognition. Despite its compact size (0.9B parameters), it achieves an NED of 0.138, outperforming the 235B-parameter Qwen3-VL by a large margin (0.382). This highlights the model’s effectiveness in handling specialized document elements.

Model	Parameters	NED (↓)
Qwen2.5-VL-72B [29]	72B	0.396
Qwen3-VL-235B-A22B-Instruct [6]	235B	0.382
PaddleOCR-VL-1.5	0.9B	0.138

Table 5 | Comparison of seal recognition performance on in-house-seal benchmark.

4.3. Inference Performance

To speed up inference, we optimize the execution workflow of PaddleOCR-VL-1.5 by introducing an asynchronous, multi-threaded design, following the same strategy adopted in PaddleOCR-VL. The entire workflow is decomposed into three consecutive stages: input preparation (primarily converting PDF pages into images), layout analysis, and VLM inference. Each stage runs in its own dedicated thread, and intermediate results are exchanged between adjacent stages via queue-based buffers. This pipelined architecture enables concurrent execution across stages, thereby increasing parallelism and improving overall throughput. For the VLM inference stage in particular, mini-batches are formed dynamically: a batch is launched either when the

queue size reaches a preset capacity or when the oldest queued item has waited longer than a specified time limit. This batching strategy makes it possible to group content blocks from multiple pages into a single inference call, which substantially increases parallel efficiency, especially when processing large collections of documents. In addition, we deploy PaddleOCR-VL-1.5-0.9B on high-performance inference and serving frameworks, i.e., FastDeploy [38], vLLM [39], and SGLang [40]. Key runtime parameters, including `max-num-batched-tokens` and `gpu-memory-utilization`, are carefully tuned to strike a balance between maximizing inference throughput and controlling GPU memory usage.

Table 6 summarizes the end-to-end inference efficiency of different OCR methods under various deployment backends on the OmniDocBench v1.5 dataset. PaddleOCR-VL-1.5 achieves the best overall performance across all metrics. With the FastDeploy backend, it reaches 1.4335 pages/s and 2016.6 tokens/s on a single NVIDIA A100 GPU, surpassing its predecessor PaddleOCR-VL by 16.9% and 18.6%, respectively. These results verify that PaddleOCR-VL-1.5 provides state-of-the-art inference speed and throughput, making it well-suited for large-scale, real-world document understanding applications.

Methods	Backend	Total Time (s)↓	Pages/s↑	Tokens/s↑
MonkeyOCR-pro-1.2B [1]	vLLM (v0.10.2)	2152.7	0.6292	949.8
dots.ocr [35]	vLLM (v0.14.0)	3236.2	0.2791	374.3
MinerU2.5 (mineru=2.5.2) [2]	vLLM (v0.10.2)	1356.5	0.9984	1415.1
DeepSeek-OCR [10]	vLLM (v0.8.5)	2130.5	0.6358	897.4
PaddleOCR-VL	vLLM (v0.10.2)	1325.5	1.0216	1419.9
PaddleOCR-VL	FastDeploy (v2.3)	1104.5	1.2261	1700.5
PaddleOCR-VL-1.5	vLLM (v0.10.2)	1184.3	1.1433	1605.6
PaddleOCR-VL-1.5	SGLang (v0.5.2)	1342.0	1.0091	1418.9
PaddleOCR-VL-1.5	FastDeploy (v2.3)	944.4	1.4335	2016.6

Table 6 | End-to-End Inference Performance Comparison on OmniDocBench v1.5. PDF documents were processed in batches of 512 on a single NVIDIA A100 GPU. The reported end-to-end runtime includes both PDF rendering and Markdown generation. All methods rely on their built-in PDF parsing modules and default DPI settings to reflect out-of-the-box performance. Tokenization and special processing details follow the protocol introduced in [9].

5. Conclusion

This work introduces PaddleOCR-VL-1.5, achieving a record SOTA accuracy of 94.5% on OmniDocBench v1.5 and demonstrating superior general precision in document parsing. A key advancement of this version is its exceptional robustness in unconstrained real-world environments. The model effectively overcomes critical hurdles such as aggressive skewing, non-rigid page warping, and erratic lighting—scenarios where traditional solutions often fail. Furthermore, it expands its functional versatility with the integration of Seal Recognition and Text Spotting. By delivering a high-fidelity data foundation, PaddleOCR-VL-1.5 will significantly enhance the reliability and performance of downstream RAG systems and Large Language Model applications in complex, real-world deployment.

References

- [1] Zhang Li, Yuliang Liu, Qiang Liu, Zhiyin Ma, Ziyang Zhang, Shuo Zhang, Zidun Guo, Jiarui Zhang, Xinyu Wang, and Xiang Bai. Monkeyocr: Document parsing with a structure-recognition-relation triplet paradigm. [arXiv preprint arXiv:2506.05218](https://arxiv.org/abs/2506.05218), 2025.

- [2] Junbo Niu, Zheng Liu, Zhuangcheng Gu, Bin Wang, Linke Ouyang, Zhiyuan Zhao, Tao Chu, Tianyao He, Fan Wu, Qintong Zhang, et al. Mineru2. 5: A decoupled vision-language model for efficient high-resolution document parsing. [arXiv preprint arXiv:2509.22186](#), 2025.
- [3] Hao Feng, Shu Wei, Xiang Fei, Wei Shi, Yingdong Han, Lei Liao, Jinghui Lu, Binghong Wu, Qi Liu, Chunhui Lin, et al. Dolphin: Document image parsing via heterogeneous anchor prompting. [arXiv preprint arXiv:2505.14059](#), 2025.
- [4] Yuan Liu, Zhongyin Zhao, Le Tian, Haicheng Wang, Xubing Ye, Yangxiu You, Zilin Yu, Chuhan Wu, Xiao Zhou, Yang Yu, et al. Points-reader: Distillation-free adaptation of vision-language models for document conversion. [arXiv preprint arXiv:2509.01215](#), 2025.
- [5] Baidu-ERNIE-Team. Ernie 4.5 technical report, 2025.
- [6] An Yang, Anfeng Li, Baosong Yang, Beichen Zhang, Binyuan Hui, Bo Zheng, Bowen Yu, Chang Gao, Chengen Huang, Chenxu Lv, et al. Qwen3 technical report. [arXiv preprint arXiv:2505.09388](#), 2025.
- [7] Josh Achiam, Steven Adler, Sandhini Agarwal, Lama Ahmad, Ilge Akkaya, Florencia Leoni Aleman, Diogo Almeida, Janko Altschmidt, Sam Altman, Shyamal Anadkat, et al. Gpt-4 technical report. [arXiv preprint arXiv:2303.08774](#), 2023.
- [8] Patrick Lewis, Ethan Perez, Aleksandra Piktus, Fabio Petroni, Vladimir Karpukhin, Naman Goyal, Heinrich Küttler, Mike Lewis, Wen-tau Yih, Tim Rocktäschel, et al. Retrieval-augmented generation for knowledge-intensive nlp tasks. [Advances in neural information processing systems](#), 33:9459–9474, 2020.
- [9] Cheng Cui, Ting Sun, Suyin Liang, Tingquan Gao, Zelun Zhang, Jiaxuan Liu, Xueqing Wang, Changda Zhou, Hongen Liu, Manhui Lin, et al. Paddleocr-vl: Boosting multilingual document parsing via a 0.9 b ultra-compact vision-language model. [arXiv preprint arXiv:2510.14528](#), 2025.
- [10] Haoran Wei, Yaofeng Sun, and Yukun Li. Deepseek-ocr: Contexts optical compression. [arXiv preprint arXiv:2510.18234](#), 2025.
- [11] Jiarui Zhang, Yuliang Liu, Zijun Wu, Guosheng Pang, Zhili Ye, Yupei Zhong, Junteng Ma, Tao Wei, Haiyang Xu, Weikai Chen, et al. Monkeyocr v1. 5 technical report: Unlocking robust document parsing for complex patterns. [arXiv preprint arXiv:2511.10390](#), 2025.
- [12] Hunyuan Vision Team, Pengyuan Lyu, Xingyu Wan, Gengluo Li, Shangpin Peng, Weinong Wang, Liang Wu, Huawen Shen, Yu Zhou, Canhui Tang, et al. Hunyuanocr technical report. [arXiv preprint arXiv:2511.19575](#), 2025.
- [13] Ting Sun, Cheng Cui, Yuning Du, and Yi Liu. Pp-doclayment: A unified document layout detection model to accelerate large-scale data construction. [arXiv preprint arXiv:2503.17213](#), 2025.
- [14] Linke Ouyang, Yuan Qu, Hongbin Zhou, Jiawei Zhu, Rui Zhang, Qunshu Lin, Bin Wang, Zhiyuan Zhao, Man Jiang, Xiaomeng Zhao, et al. Omnidocbench: Benchmarking diverse pdf document parsing with comprehensive annotations. In [Proceedings of the Computer Vision and Pattern Recognition Conference](#), pages 24838–24848, 2025.
- [15] Google DeepMind. Gemini 3.0. <https://blog.google/products-and-platforms/products/gemini/gemini-3-collection/>, 2025.

- [16] Yian Zhao, Wenyu Lv, Shangliang Xu, Jinman Wei, Guanzhong Wang, Qingqing Dang, Yi Liu, and Jie Chen. Detsr beat yolos on real-time object detection. In Proceedings of the IEEE/CVF conference on computer vision and pattern recognition, pages 16965–16974, 2024.
- [17] Mostafa Dehghani, Basil Mustafa, Josip Djolonga, Jonathan Heek, Matthias Minderer, Mathilde Caron, Andreas Steiner, Joan Puigcerver, Robert Geirhos, Ibrahim M Alabdulmohsin, et al. Patch n’pack: Navit, a vision transformer for any aspect ratio and resolution. Advances in Neural Information Processing Systems, 36:2252–2274, 2023.
- [18] PaddlePaddle Authors. Paddleformers. <https://github.com/PaddlePaddle/PaddleFormers>, 2025.
- [19] Yanjun Ma, Dianhai Yu, Tian Wu, and Haifeng Wang. Paddlepaddle: An open-source deep learning platform from industrial practice. Frontiers of Data and Computing, 1(1):105–115, 2019.
- [20] Zhihong Shao, Peiyi Wang, Qihao Zhu, Runxin Xu, Junxiao Song, Xiao Bi, Haowei Zhang, Mingchuan Zhang, YK Li, Yang Wu, et al. Deepseekmath: Pushing the limits of mathematical reasoning in open language models. arXiv preprint arXiv:2402.03300, 2024.
- [21] Alec Radford, Jong Wook Kim, Chris Hallacy, Aditya Ramesh, Gabriel Goh, Sandhini Agarwal, Girish Sastry, Amanda Askell, Pamela Mishkin, Jack Clark, et al. Learning transferable visual models from natural language supervision. In International conference on machine learning, pages 8748–8763. PmLR, 2021.
- [22] Cheng Cui, Ting Sun, Manhui Lin, Tingquan Gao, Yubo Zhang, Jiakuan Liu, Xueqing Wang, Zelun Zhang, Changda Zhou, Hongen Liu, et al. Paddleocr 3.0 technical report. arXiv preprint arXiv:2507.05595, 2025.
- [23] Bin Wang, Fan Wu, Linke Ouyang, Zhuangcheng Gu, Rui Zhang, Renqiu Xia, Botian Shi, Bo Zhang, and Conghui He. Image over text: Transforming formula recognition evaluation with character detection matching. In Proceedings of the IEEE/CVF Conference on Computer Vision and Pattern Recognition (CVPR), pages 19681–19690, June 2025.
- [24] Vik Paruchuri. Marker. <https://github.com/datalab-to/marker>, 2025. Accessed: 2025-09-25.
- [25] opendatalab. Mineru2.0-2505-0.9b. <https://huggingface.co/opendatalab/MinerU2.0-2505-0.9B>, 2025.
- [26] Jinguo Zhu, Weiyun Wang, Zhe Chen, Zhaoyang Liu, Shenglong Ye, Lixin Gu, Hao Tian, Yuchen Duan, Weijie Su, Jie Shao, et al. Internvl3: Exploring advanced training and test-time recipes for open-source multimodal models. arXiv preprint arXiv:2504.10479, 2025.
- [27] Weiyun Wang, Zhangwei Gao, Lixin Gu, Hengjun Pu, Long Cui, Xingguang Wei, Zhaoyang Liu, Linglin Jing, Shenglong Ye, Jie Shao, et al. Internvl3. 5: Advancing open-source multimodal models in versatility, reasoning, and efficiency. arXiv preprint arXiv:2508.18265, 2025.
- [28] OpenAI. Gpt-5.2 system card, 2025. URL https://cdn.openai.com/pdf/3a4153c8-c748-4b71-8e31-aecbde944f8d/oai_5_2_system-card.pdf.

- [29] Shuai Bai, Keqin Chen, Xuejing Liu, Jialin Wang, Wenbin Ge, Siboz Song, Kai Dang, Peng Wang, Shijie Wang, Jun Tang, et al. Qwen2. 5-vl technical report. [arXiv preprint arXiv:2502.13923](https://arxiv.org/abs/2502.13923), 2025.
- [30] Google DeepMind. Gemini 2.5. <https://blog.google/technology/google-deepmind/gemini-model-thinking-updates-march-2025/>, 2025.
- [31] chatdoc com. Ocrflux. <https://github.com/chatdoc-com/OCRFlux>, 2025. Accessed:2025-09-25.
- [32] Mistral AI Team. Mistral-ocr. https://mistral.ai/news/mistral-ocr?utm_source=ai-bot.cn, 2025.
- [33] Jake Poznanski, Jon Borchardt, Jason Dunkelberger, Regan Huff, Daniel Lin, Aman Rangapur, Christopher Wilhelm, Kyle Lo, and Luca Soldaini. olmocr: Unlocking trillions of tokens in pdfs with vision language models. [arXiv preprint arXiv:2502.18443](https://arxiv.org/abs/2502.18443), 2025.
- [34] Souvik Mandal, Ashish Talewar, Paras Ahuja, and Prathamesh Juvatkar. Nanonets-ocr-s: A model for transforming documents into structured markdown with intelligent content recognition and semantic tagging, 2025.
- [35] rednote-hilab. dots.ocr: Multilingual document layout parsing in a single vision-language model, 2025.
- [36] Changda Zhou, Ziyue Gao, Xueqing Wang, Tingquan Gao, Cheng Cui, Jing Tang, and Yi Liu. Real5-omnidocbench: A full-scale physical reconstruction benchmark for robust document parsing in the wild, 2026. URL <https://arxiv.org/abs/2603.04205>.
- [37] Qing Jiang, Junan Huo, Xingyu Chen, Yuda Xiong, Zhaoyang Zeng, Yihao Chen, Tianhe Ren, Junzhi Yu, and Lei Zhang. Detect anything via next point prediction. [arXiv preprint arXiv:2510.12798](https://arxiv.org/abs/2510.12798), 2025.
- [38] PaddlePaddle Authors. Fastdeploy. <https://github.com/PaddlePaddle/FastDeploy>, 2025.
- [39] Woosuk Kwon, Zhuohan Li, Siyuan Zhuang, Ying Sheng, Lianmin Zheng, Cody Hao Yu, Joseph Gonzalez, Hao Zhang, and Ion Stoica. Efficient memory management for large language model serving with pagedattention. In [Proceedings of the 29th symposium on operating systems principles](https://doi.org/10.1145/3613907.3614007), pages 611–626, 2023.
- [40] Lianmin Zheng, Liangsheng Yin, Zhiqiang Xie, Chuyue Livia Sun, Jeff Huang, Cody Hao Yu, Shiyi Cao, Christos Kozyrakis, Ion Stoica, Joseph E Gonzalez, et al. Sglang: Efficient execution of structured language model programs. [Advances in neural information processing systems](https://doi.org/10.1145/3655577.3655700), 37:62557–62583, 2024.

Appendix

A. Comparison of PaddleOCR-VL-1.5 and 1.0 Models

Category	Capability Item	V1	V1.5	V1.5 Description
Fundamental	Layout Analysis	★★☆☆☆	★★★★☆	Improved stability for warped/skewed scenes; added CAD and comics.
	Text Recognition	★★★★☆	★★★★★	Gains in vertical text, special characters, and emphasis marks.
	Table Recognition	★★★★☆	★★★★☆	Improvements for borderless tables and invoices.
	Formula Recognition	★★★★☆	★★★★☆	Better in skewed formulas and illumination scenarios.
	Chart Recognition	★★★★☆	★★★★☆	Capability remains consistent with the previous version.
	Reading Order	★★★★☆	★★★★☆	Significant boost for irregular layouts.
Adaptability	Skewed Docs	☆☆☆☆☆	★★★★★	Dramatic improvement for high-angle tilted documents.
	Scanned Docs	★★★★☆	★★★★★	Stability for low-quality scans is significantly enhanced.
	Warped Docs	★★☆☆☆	★★★★★	Supports complex physical deformation and folded paper.
	Screen Photo	★★☆☆☆	★★★★★	Suppresses interference from reflections and Moiré patterns.
	Illumination	★★★★☆	★★★★★	Superior performance in uneven or weak lighting.
New Features	Seal Recognition	☆☆☆☆☆	★★★★☆	Recognition of various official seals and stamps.
	Text Spotting	☆☆☆☆☆	★★★★☆	Localization and recognition of multiple character sets.
	Cross-page Table Merginig	☆☆☆☆☆	★★★★☆	Merges split tables while maintaining consistency.
	Heading Hierarchy	☆☆☆☆☆	★★★☆☆	Title hierarchy recognition across multi-page documents.

Table A1 | Comprehensive functional evolution and robustness comparison between PaddleOCR-VL and PaddleOCR-VL-1.5. The star ratings only indicate the relative performance of the two versions and do not represent their absolute accuracy.

B. Details of the Real5-OmniDocBench Benchmark

Real5-OmniDocBench¹ is a brand-new benchmark oriented toward real-world scenarios, which we constructed based on the OmniDocBench v1.5 [14] dataset. PaddleOCR-VL-1.5 achieves state-of-the-art (SOTA) results across all sub-scenarios within Real5-OmniDocBench, demonstrating its robust parsing capabilities for real-world documents. A detailed comparison of PaddleOCR-VL-1.5 against other advanced document parsing models across various metrics on this dataset is provided in this Appendix.

As shown in Table A2, under the scanning scenario, PaddleOCR-VL-1.5 achieves state-of-the-art performance across all key metrics, consistently outperforming existing pipeline tools, general vision-language models, and specialized document parsing models. Compared to its predecessor, PaddleOCR-VL, the new version maintains a compact parameter size of 0.9B while raising the overall score from 92.11% to a leading 93.43%. Notably, PaddleOCR-VL-1.5 sets new records in all sub-tasks within this scenario, including a Formula-CDM score of 93.04% and a Table-TEDS score of 90.97%, both significantly surpassing larger models such as Qwen3-VL-235B and Gemini-3 Pro. Additionally, the model achieves exceptionally low Text-Edit Distance (0.037) and Reading Order score (0.045), further demonstrating its high accuracy in text recognition, formula extraction, and complex table structure analysis. Overall, PaddleOCR-VL-1.5 delivers a new breakthrough in the Real5-OmniDocBench-scanning scenario.

Model Type	Methods	Parameters	Overall \uparrow	Text ^{Edit} \downarrow	Formula ^{CDM} \uparrow	Table ^{TEDS} \uparrow	Reading Order ^{Edit} \downarrow
Pipeline Tools	Maker-1.8.2 [24]	-	70.27	0.223	77.03	56.05	0.238
	PP-StructureV3 [22]	-	84.68	0.094	84.34	79.06	0.092
General VLMs	GPT-5.2 [28]	-	84.43	0.142	85.68	81.78	0.109
	Qwen2.5-VL-72B [29]	72B	86.19	0.110	86.14	83.41	0.114
	Gemini-2.5 Pro [30]	-	89.25	0.073	87.44	87.62	0.098
	Qwen3-VL-235B-A22B-Instruct [29]	235B	89.43	0.059	89.01	85.19	0.066
	Gemini-3 Pro [15]	-	89.47	0.071	88.16	87.37	0.078
Specialized VLMs	Dolphin [3]	322M	72.16	0.154	64.58	67.27	0.130
	Dolphin-1.5 [3]	0.3B	83.39	0.097	76.25	83.65	0.090
	MinerU2-VLM [25]	0.9B	83.60	0.094	79.76	80.44	0.091
	MonkeyOCR-pro-1.2B [1]	1.9B	84.64	0.123	84.17	82.13	0.145
	MonkeyOCR-3B [1]	3.7B	84.65	0.100	84.16	79.81	0.143
	Nanonets-OCR-s [34]	3B	85.52	0.106	88.09	79.11	0.106
	Deepseek-OCR [10]	3B	86.17	0.078	83.59	82.69	0.085
	dots.ocr [35]	3B	86.87	0.083	83.27	85.68	0.081
	MonkeyOCR-pro-3B [1]	3.7B	86.94	0.103	86.29	84.86	0.141
	MinerU2.5 [2]	1.2B	90.06	0.052	88.22	87.16	0.050
	PaddleOCR-VL [9]	0.9B	92.11	0.039	90.35	89.90	0.048
	PaddleOCR-VL-1.5	0.9B	93.43	0.037	93.04	90.97	0.045

Table A2 | Comprehensive evaluation of document parsing on Real5-OmniDocBench-scanning

As shown in Table A3, PaddleOCR-VL-1.5 exhibits notable robustness in the warping scenario, achieving an overall score of 91.25%, which is higher than the larger Qwen3-VL-235B model (89.99%). Its Formula-CDM score of 90.94% and Table-TEDS score of 88.10% indicate a strong ability to preserve document structure under significant geometric distortion.

¹<https://huggingface.co/datasets/PaddlePaddle/Real5-OmniDocBench>

Model Type	Methods	Parameters	Overall↑	Text ^{Edit} ↓	Formula ^{CDM} ↑	Table ^{TEDS} ↑	Reading Order ^{Edit} ↓
Pipeline Tools	Maker-1.8.2 [24]	-	58.98	0.349	72.71	39.08	0.390
	PP-StructureV3 [22]	-	59.34	0.376	68.22	47.40	0.261
General VLMs	GPT-5.2 [28]	-	76.26	0.239	80.90	71.80	0.165
	Gemini-2.5 Pro [30]	-	87.63	0.092	86.50	85.59	0.109
	Qwen2.5-VL-72B [29]	72B	87.77	0.086	88.85	83.06	0.102
	Gemini-3 Pro [15]	-	88.90	0.086	88.10	87.20	0.087
	Qwen3-VL-235B-A22B-Instruct [29]	235B	89.99	0.051	89.06	85.95	0.064
Specialized VLMs	Dolphin-1.5 [3]	0.3B	50.50	0.383	47.24	42.52	0.309
	Dolphin [3]	322M	60.35	0.316	61.06	51.58	0.247
	Deepseek-OCR [10]	3B	67.20	0.328	73.59	60.80	0.226
	MinerU2-VLM [25]	0.9B	73.73	0.202	77.72	63.65	0.173
	MonkeyOCR-pro-1.2B [1]	1.9B	76.59	0.196	78.85	70.52	0.221
	MonkeyOCR-3B [1]	3.7B	77.27	0.164	79.08	69.18	0.211
	MonkeyOCR-pro-3B [1]	3.7B	78.90	0.168	79.55	73.94	0.212
	Nanonets-OCR-s [34]	3B	83.56	0.121	86.24	76.57	0.124
	MinerU2.5 [2]	1.2B	83.76	0.154	85.92	80.71	0.104
	PaddleOCR-VL [9]	0.9B	85.97	0.093	85.45	81.77	0.092
	dots.ocr [35]	3B	86.01	0.087	85.03	81.74	0.093
	PaddleOCR-VL-1.5	0.9B	91.25	0.053	90.94	88.10	0.063

Table A3 | Comprehensive evaluation of document parsing on Real5-OmniDocBench-warping.

In the screen photography scenario presented in Table A4, PaddleOCR-VL-1.5 attains an overall score of 91.76%, demonstrating competitive performance among specialized vision-language models. The model achieves a Formula-CDM score of 90.88%, outperforming MinerU2.5 (87.55%) and dots.ocr (85.34%), and shows effective handling of Moire patterns and reflections typically encountered in screen-captured documents.

Model Type	Methods	Parameters	Overall↑	Text ^{Edit} ↓	Formula ^{CDM} ↑	Table ^{TEDS} ↑	Reading Order ^{Edit} ↓
Pipeline Tools	Maker-1.8.2 [24]	-	63.65	0.290	72.73	47.21	0.325
	PP-StructureV3 [22]	-	66.89	0.204	73.26	47.82	0.165
General VLMs	GPT-5.2 [28]	-	76.75	0.208	79.27	71.73	0.148
	Qwen2.5-VL-72B [29]	72B	86.48	0.100	87.46	82.00	0.102
	Gemini-2.5 Pro [30]	-	87.11	0.103	85.30	86.31	0.117
	Gemini-3 Pro [15]	-	88.86	0.084	87.33	87.65	0.087
	Qwen3-VL-235B-A22B-Instruct [29]	235B	89.27	0.068	88.72	85.85	0.071
Specialized VLMs	Dolphin [3]	322M	64.29	0.232	58.66	57.38	0.195
	Dolphin-1.5 [3]	0.3B	69.76	0.205	61.80	68.00	0.177
	Deepseek-OCR [10]	3B	75.31	0.220	77.68	70.26	0.169
	MinerU2-VLM [25]	0.9B	78.77	0.139	79.02	71.17	0.123
	MonkeyOCR-pro-1.2B [1]	1.9B	80.24	0.148	80.78	74.74	0.179
	MonkeyOCR-3B [1]	3.7B	80.71	0.122	81.33	73.04	0.177
	MonkeyOCR-pro-3B [1]	3.7B	82.44	0.124	81.55	78.13	0.177
	PaddleOCR-VL [9]	0.9B	82.54	0.103	83.58	74.36	0.107
	Nanonets-OCR-s [34]	3B	84.86	0.112	86.65	79.09	0.117
	dots.ocr [35]	3B	87.18	0.081	85.34	84.26	0.079
	MinerU2.5 [2]	1.2B	89.41	0.062	87.55	86.83	0.053
	PaddleOCR-VL-1.5	0.9B	91.76	0.050	90.88	89.38	0.059

Table A4 | Comprehensive evaluation of document parsing on Real5-OmniDocBench-screen-photography.

Table A5 evaluates performance under illumination variations, where PaddleOCR-VL-1.5 reaches an overall score of 92.16%. This result not only marks a significant improvement over the previous PaddleOCR-VL (89.61%) but also surpasses top-tier general VLMs such as Gemini-3 Pro (89.53%). The model’s Formula-CDM score of 91.80% and Table-TEDS of 89.33% underscore

its high sensitivity and accuracy in low-contrast or unevenly lit environments.

Model Type	Methods	Parameters	Overall \uparrow	Text ^{Edit} \downarrow	Formula ^{CDM} \uparrow	Table ^{TEDS} \uparrow	Reading Order ^{Edit} \downarrow
Pipeline Tools	Maker-1.8.2 [24]	-	66.31	0.259	74.80	50.03	0.337
	PP-StructureV3 [22]	-	73.38	0.158	77.75	58.19	0.126
General VLMs	GPT-5.2 [28]	-	80.88	0.191	84.41	77.37	0.134
	Qwen2.5-VL-72B [29]	72B	87.25	0.087	86.44	84.03	0.097
	Gemini-2.5 Pro [30]	-	87.97	0.083	86.13	86.11	0.103
	Qwen3-VL-235B-A22B-Instruct [29]	235B	89.27	0.060	87.81	86.05	0.070
	Gemini-3 Pro [15]	-	89.53	0.073	87.78	88.14	0.080
Specialized VLMs	Dolphin [3]	322M	67.29	0.197	61.42	60.10	0.173
	Dolphin-1.5 [3]	0.3B	75.61	0.159	70.04	72.69	0.133
	Deepseek-OCR [10]	3B	78.10	0.192	81.71	71.81	0.156
	MinerU2-VLM [25]	0.9B	80.51	0.135	80.72	74.29	0.123
	MonkeyOCR-pro-1.2B [1]	1.9B	82.11	0.144	82.07	78.67	0.172
	MonkeyOCR-3B [1]	3.7B	83.16	0.118	83.63	77.62	0.168
	MonkeyOCR-pro-3B [1]	3.7B	84.71	0.120	84.13	82.02	0.171
	Nanonets-OCR-s [34]	3B	85.01	0.099	87.94	76.96	0.112
	dots.ocr [35]	3B	87.57	0.068	85.07	84.44	0.076
	MinerU2.5 [2]	1.2B	89.57	0.065	88.36	86.87	0.062
	PaddleOCR-VL [9]	0.9B	89.61	0.049	86.66	87.02	0.055
	PaddleOCR-VL-1.5	0.9B	92.16	0.046	91.80	89.33	0.051

Table A5 | Comprehensive evaluation of document parsing on Real5-OmniDocBench-illumination.

Under the challenging skew detailed in Table A6, PaddleOCR-VL-1.5 maintains its dominance with an overall score of 91.66%, once again outperforming general VLMs including Gemini-3 Pro (89.45%). It particularly excels in complex structural recovery, evidenced by a Table-TEDS score of 91.00% and a Text-Edit distance reduced to 0.047, demonstrating its superior ability to rectify and parse slanted document layouts.

Model Type	Methods	Parameters	Overall \uparrow	Text ^{Edit} \downarrow	Formula ^{CDM} \uparrow	Table ^{TEDS} \uparrow	Reading Order ^{Edit} \downarrow
Pipeline Tools	PP-StructureV3 [22]	-	37.98	0.557	44.37	25.27	0.417
	Maker-1.8.2 [24]	-	41.27	0.536	60.16	17.23	0.543
General VLMs	GPT-5.2 [28]	-	75.00	0.257	80.27	70.47	0.167
	Qwen3-VL-235B-A22B-Instruct [29]	235B	86.56	0.077	83.96	83.41	0.091
	Qwen2.5-VL-72B [29]	72B	86.90	0.077	87.26	81.14	0.091
	Gemini-2.5 Pro [30]	-	89.07	0.077	87.89	86.99	0.104
	Gemini-3 Pro [15]	-	89.45	0.080	88.33	88.06	0.092
Specialized VLMs	Dolphin-1.5 [3]	0.3B	28.16	0.553	25.60	14.18	0.419
	Dolphin [3]	322M	44.83	0.500	51.34	33.22	0.321
	MonkeyOCR-pro-1.2B [1]	1.9B	62.18	0.292	66.25	49.46	0.317
	Deepseek-OCR [10]	3B	63.01	0.327	73.27	48.48	0.231
	MonkeyOCR-pro-3B [1]	3.7B	64.47	0.251	69.06	49.42	0.301
	MonkeyOCR-3B [1]	3.7B	65.67	0.248	69.23	52.59	0.300
	MinerU2-VLM [25]	0.9B	68.16	0.230	74.45	53.07	0.191
	MinerU2.5 [2]	1.2B	75.24	0.305	81.78	74.39	0.151
	PaddleOCR-VL [9]	0.9B	77.47	0.192	78.81	72.83	0.193
	Nanonets-OCR-s [34]	3B	81.98	0.121	85.78	72.22	0.133
	dots.ocr [35]	3B	84.27	0.087	85.73	75.74	0.094
	PaddleOCR-VL-1.5	0.9B	91.66	0.047	91.00	88.69	0.061

Table A6 | Comprehensive evaluation of document parsing on Real5-OmniDocBench-skewing variation.

C. Supported Languages

PaddleOCR-VL-1.5 supports a total of 111 languages. Compared to PaddleOCR-VL, PaddleOCR-VL-1.5 adds recognition capabilities for China’s Tibetan script and Bengali. Table A7 lists the correspondence between each language category and the specific supported languages/scripts.

Language Category	Specific Languages
Chinese	Chinese
English	English
Korean	Korean
Japanese	Japanese
Thai	Thai
Greek	Greek
Tamil	Tamil
Telugu	Telugu
Bengali*	Bengali*
China’s Tibetan script*	China’s Tibetan script*
Arabic	Arabic, Persian, Uyghur, Urdu, Pashto, Kurdish, Sindhi, Balochi
Latin	French, German, Afrikaans, Italian, Spanish, Bosnian, Portuguese, Czech, Welsh, Danish, Estonian, Irish, Croatian, Uzbek, Hungarian, Serbian (Latin), Indonesian, Occitan, Icelandic, Lithuanian, Maori, Malay, Dutch, Norwegian, Polish, Slovak, Slovenian, Albanian, Swedish, Swahili, Tagalog, Turkish, Latin, Azerbaijani, Kurdish, Latvian, Maltese, Pali, Romanian, Vietnamese, Finnish, Basque, Galician, Luxembourgish, Romansh, Catalan, Quechua
Cyrillic	Russian, Belarusian, Ukrainian, Serbian (Cyrillic), Bulgarian, Mongolian, Abkhazian, Adyghe, Kabardian, Avar, Dargin, Ingush, Chechen, Lak, Lezgin, Tabasaran, Kazakh, Kyrgyz, Tajik, Macedonian, Tatar, Chuvash, Bashkir, Malian, Moldovan, Udmurt, Komi, Ossetian, Buryat, Kalmyk, Tuvan, Sakha, Karakalpak
Devanagari	Hindi, Marathi, Nepali, Bihari, Maithili, Angika, Bhojpuri, Magahi, Santali, Newari, Konkani, Sanskrit, Haryanvi

Table A7 | Supported Languages/scripts (*indicates newly added languages/scripts)

D. Inference Performance on Different Hardware Configurations

We evaluated the inference throughput and latency of PaddleOCR-VL-1.5 across multiple hardware configurations, with the detailed results presented in Table A8. In our experiments, all PDF pages are rendered at 72 DPI, which provides a good trade-off between memory efficiency and the visual fidelity required for reliable OCR. We note that the experiments on different hardware platforms were conducted without extensive parameter tuning or system-level optimization; therefore, the reported performance figures should be regarded as conservative and still leave room for further improvement. All models were evaluated using three deployment backends, namely FastDeploy v2.3.0, vLLM v0.10.2, and SGLang v0.5.2. Across these frameworks, PaddleOCR-VL-1.5 consistently delivers high and stable inference efficiency, demonstrating strong generalization across diverse hardware configurations and execution engines, as well as good compatibility with heterogeneous computing environments.

Hardware	Backend	Total Time (s)↓	Pages/s↑	Tokens/s↑	Avg. VRAM Usage (GB)↓
H800	FastDeploy	556.4	2.4320	3404.5	64.8
	vLLM	761.8	1.7772	2488.0	46.2
	SGLang	868.5	1.5589	2185.2	48.9
A100	FastDeploy	671.3	2.0160	2826.0	62.1
	vLLM	981.4	1.3797	1926.1	43.5
	SGLang	1100.9	1.2301	1722.5	48.9
H20	FastDeploy	743.7	1.8206	2545.0	77.2
	vLLM	796.1	1.7007	2382.0	75.0
	SGLang	862.2	1.5702	2204.5	74.3
L20	FastDeploy	845.0	1.6023	2248.4	41.0
	vLLM	998.2	1.3565	1890.7	25.1
	SGLang	1126.8	1.2018	1680.7	30.2
A10	FastDeploy	1179.9	1.1477	1607.8	21.8
	vLLM	1245.5	1.0873	1520.6	13.5
	SGLang	1504.3	0.9003	1260.1	19.0
RTX 3060	vLLM	2531.8	0.5351	748.1	11.8
	SGLang	2587.7	0.5235	730.5	11.7
RTX 4090D	vLLM	923.5	1.4667	2040.1	16.3
	SGLang	1079.5	1.2548	1750.9	20.0

Table A8 | End-to-End Inference Performance

E. Real-world Samples

This appendix demonstrates the robustness and versatility of PaddleOCR-VL-1.5 in processing diverse, high-complexity real-world scenarios.

Section E.1 demonstrates the real-world document parsing capability of PaddleOCR-VL-1.5. Figures A1–A5 demonstrate the robust performance of PaddleOCR-VL-1.5 to parse real-world documents across diverse conditions, including varying illumination, geometric skew, screen-to-photo noise, and warped scanned surfaces.

Figures A6–A9 in Section E.2 illustrate the robustness of PaddleOCR-VL-1.5 in layout analysis across challenging real-world conditions, including skewed or curved geometries, screen-to-photo noise, and illumination variations. Furthermore, Figure A10 highlights its extended generalizability to specialized domains—such as comics, CAD drawings, and multi-stamped documents—where earlier version of the model faced limitations.

Section E.3 evaluates the text recognition performance of PaddleOCR-VL-1.5 under diverse constraints. As shown in Figure A11, the model exhibits improved sensitivity to text decorations, including underlines, emphasis marks, and wavy patterns, surpassing its predecessor. Figure A12 and Figure A13 demonstrate enhanced robustness in identifying special characters and long-tail cases, such as vertical orientations and character-level ambiguities.

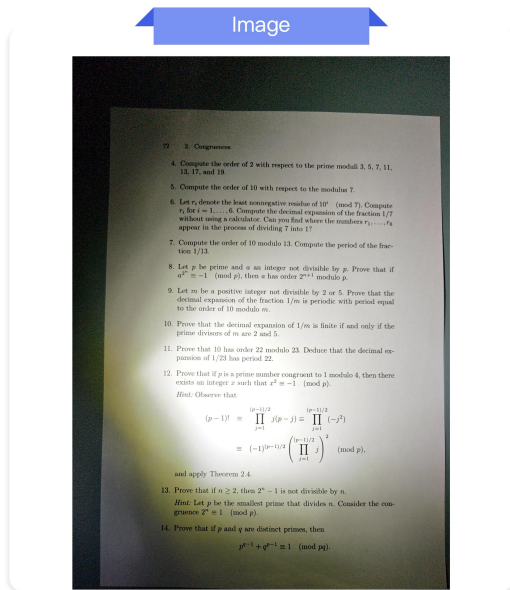
The model’s table recognition abilities are demonstrated in section E.4. Figure A14 illustrates the robustness of the model in processing complex layouts, including tables from academic textbooks and those containing embedded images or mathematical formulas. The proficiency of the model in multilingual table recognition is presented in Figure A15. Furthermore, Figure A16 demonstrates its extended capability for cross-page table detection and merging, addressing the challenges of multi-page document parsing."

Figures in section E.5 detail the formula recognition performance. As illustrated in Figure A17, the updated model exhibits superior performance in mathematical expression recognition, specifically regarding sub/superscript accuracy, multi-line formula segmentation, and a lower overall error rate.

In section E.6, seal recognition represents a novel capability of this model update. As illustrated in Figures A18–A20, the model accurately extracts content from various types of seals, demonstrating high precision even when faced with complex background interference and cluttered environments.

Figure A21 in section E.7 highlights the newly integrated text spotting capability of the model, which enables simultaneous localization and recognition. The results demonstrate superior robustness across challenging layouts, ranging from multi-column magazine pages and complex tables to irregular handwritten content.

E.1. Real-word Document Parsing



PaddleOCR-VL-1.5

4. Compute the order of 2 with respect to the prime moduli 3, 5, 7, 11, 13, 17, and 19.

5. Compute the order of 10 with respect to the modulus 7.

6. Let r_i denote the least nonnegative residue of $10^i \pmod{7}$. Compute r_i for $i = 1, \dots, 6$. Compute the decimal expansion of the fraction $1/7$ without using a calculator. Can you find where the numbers r_1, \dots, r_6 appear in the process of dividing 7 into 1?

7. Compute the order of 10 modulo 13. Compute the period of the fraction $1/13$.

8. Let p be prime and a an integer not divisible by p . Prove that if $a^{p-1} \equiv -1 \pmod{p}$, then a has order 2^{k+1} modulo p .

9. Let m be a positive integer not divisible by 2 or 5. Prove that the decimal expansion of the fraction $1/m$ is periodic with period equal to the order of 10 modulo m .

10. Prove that the decimal expansion of $1/m$ is finite if and only if the prime divisors of m are 2 and 5.

11. Prove that 10 has order 22 modulo 23. Deduce that the decimal expansion of $1/23$ has period 22.

12. Prove that if p is a prime number congruent to 1 modulo 4, then there exists an integer x such that $x^2 \equiv -1 \pmod{p}$.

Hint: Observe that

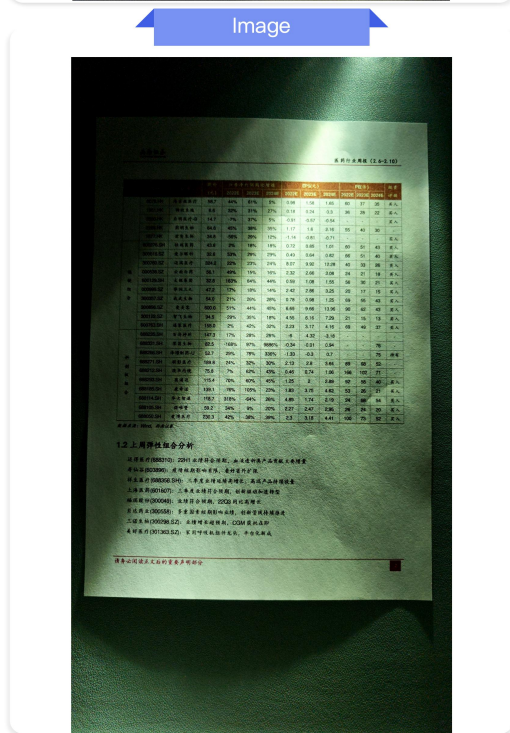
$$(p-1)! \equiv \prod_{j=1}^{(p-1)/2} j(p-j) \equiv \prod_{j=1}^{(p-1)/2} (-j^2) \equiv (-1)^{(p-1)/2} \left(\prod_{j=1}^{(p-1)/2} j \right)^2 \pmod{p},$$

and apply Theorem 2.4.

13. Prove that if $n \geq 2$, then $2^n - 1$ is not divisible by n .

Hint: Let p be the smallest prime that divides n . Consider the congruence $2^p \equiv 1 \pmod{p}$.

14. Prove that if p and q are distinct primes, then

$$p^{q-1} + q^{p-1} \equiv 1 \pmod{pq}.$$


PaddleOCR-VL-1.5

Table with columns: 股价, 归母净利润同比增长, EPS(元), PE(倍), 投资评级

60076.HK 博济医药 58.7 44% 69% 6% 0.98 1.58 1.65 60 37 35 买入

13651.HK 翰宇生物 6.6 32% 31% 27% 0.16 0.24 0.3 36 28 22 买入

2503.HK 血药集团 14.7 -7% 37% 5% -0.91 -0.57 -0.54 - - - 买入

3203.HK 药明生物 64.6 45% 38% 30% 1.17 1.6 2.16 55 40 30 -

6077.HK 药明康德 34.6 -55% 29% 62% 1.14 -0.61 -0.71 - - - 买入

600276.SH 恒瑞医药 43.6 2% 19% 16% 0.72 0.65 1.01 60 51 43 买入

300152.SZ 爱尔眼科 32.6 53% 29% 29% 0.48 0.64 0.82 66 51 40 买入

300760.SZ 迈瑞医疗 334.2 22% 23% 24% 8.07 8.92 12.28 40 33 26 买入

000538.SZ 云南白药 56.1 49% 15% 16% 3.2 2.66 3.08 24 21 18 买入

300729.SZ 太辰集团 32.8 163% 84% 44% 0.59 1.08 1.55 56 30 21 买入

000999.SZ 华谊兄弟 47.2 17% 18% 14% 2.42 2.86 3.25 20 17 15 买入

300357.SZ 联众股份 54.0 21% 26% 28% 0.78 0.88 1.25 69 55 43 买入

300895.SZ 美泰集团 600.0 51% 44% 45% 6.69 9.66 13.95 90 62 43 买入

301022.SZ 智飞生物 94.5 -29% 30% 18% 4.55 6.16 7.29 21 15 13 买入

600763.SH 通策医疗 155.0 2% 42% 32% 2.23 3.17 4.16 69 49 37 买入

688235.SH 西药神州 147.3 17% 28% 20% -6 -4.32 -3.18 - - - -

688335.SH 蓝晶半导体 82.5 -16% 97% 98% -0.34 -0.01 0.94 - - - 76 -

688266.SH 博济医药 52.7 29% 78% 336% -1.33 -0.3 0.7 - - - 75 持有

688271.SH 联众股份 189.8 24% 32% 30% 2.13 2.8 3.64 89 68 52 -

688272.SH 瀚宇内德 75.8 7% 62% 43% 0.46 0.74 1.06 166 102 71 -

688293.SH 奥康医疗 115.4 70% 60% 45% 1.25 2 2.89 92 58 40 买入

688165.SH 康希诺 126.1 -76% 105% 23% 1.83 3.75 4.62 53 26 21 买入

688162.SH 华大基因 188.7 39% -64% 28% 4.89 1.74 2.19 24 68 94 买入

688105.SH 康泰生物 53.2 34% 9% 20% 2.27 2.47 2.66 26 24 20 买入

688050.SH 曼迪药业 236.3 42% 36% 59% 2.3 3.16 4.41 100 73 62 买入

数据来源: Wind, 西南证券

1.2 上周弹性组合分析

投资组合(688110): 22H1业绩超预期, 血液制品产品放量主要增量

持仓组合(688110): 恒瑞医药(600276)、翰宇生物(13651.HK)、血药集团(2503.HK)、药明生物(3203.HK)、药明康德(6077.HK)、恒瑞医药(600276)、恒瑞医药(600276)、恒瑞医药(600276)

持仓组合(688266): 三季报业绩超预期, 血液制品产品放量

持仓组合(688271): 三季报业绩超预期, 血液制品产品放量

持仓组合(688293): 三季报业绩超预期, 血液制品产品放量

持仓组合(688165): 三季报业绩超预期, 血液制品产品放量

持仓组合(688162): 三季报业绩超预期, 血液制品产品放量

持仓组合(688105): 三季报业绩超预期, 血液制品产品放量

持仓组合(688050): 三季报业绩超预期, 血液制品产品放量

Figure A1 | The Markdown Output for Illumination.

Image



PaddleOCR-VL-1.5

第三章 产业区位选择

思考

举例说明其他

因素是如何影响工

业区位的。

动力充足的动力是工业生产的必要条件。对于需要消耗大量能源的工业，例如炼铝工业等，需布局在能源的供应地。

环境条件 不同工业对环境条件有着不同的要求。如酿酒业需要优质的水源，电子工业需要清洁的环境等。有些企业在生产过程中，会造成大气污染、水污染和固体废弃物污染等，影响人类的生产和生活，因此工业布局也要考虑对环境的影响。

其他因素 除了上述因素，政策、个人喜好或特殊关系等也会对工业区位产生影响。例如政府通过法规、税收、用地、交通和基础设施等方面政策影响工业的生产和分布。某些企业家的个人喜好或特殊关系，也会影响工厂的选址。

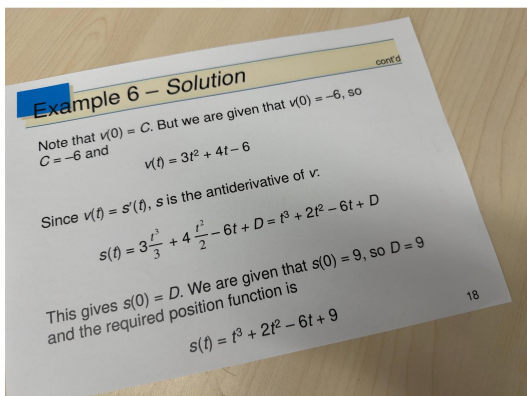
案例研究 汽车厂选址

2014年底，北汽集团与河北省政府签署协议，将北京现代汽车公司第四工厂的选址确定在沧州市。



图 3-2-4 沧州市在河北省的位置示意图 1:8 200 000

Image



PaddleOCR-VL-1.5

Example 6 – Solution

cont'd

Note that $v(0) = C$. But we are given that $v(0) = -6$, so $C = -6$ and

$$v(t) = 3t^2 + 4t - 6$$

Since $v(t) = s'(t)$, s is the antiderivative of v .

$$s(t) = 3 \frac{t^3}{3} + 4 \frac{t^2}{2} - 6t + D = t^3 + 2t^2 - 6t + D$$

This gives $s(0) = D$. We are given that $s(0) = 9$, so $D = 9$ and the required position function is

$$s(t) = t^3 + 2t^2 - 6t + 9$$

Figure A2 | The Markdown Output for Skew.

Image



PaddleOCR-VL-1.5

Automation technologies can be broadly grouped into three categories:

1. Robotic Process Automation (RPA): The simplest form of automation, RPA technology automates repetitive rule-based processes. This technology cannot learn, adapt or make decisions; an RPA bot simply applies a consistent set of rules to a process to deliver quick and efficient outcomes. Many manual administrative processes can be streamlined in this way.
2. Machine learning: At the next level is machine learning, where a computer is able to use large volumes of data to understand and predict the desired course of action, with performance improving over time. Chat-bots are a good example of machine learning being used today in the financial sector. These bots use technologies such as natural language processing (NLP) to communicate in real time with human customers, use data from past interactions to understand the nature of the customer's query, and provide the desired information or response.
3. Cognitive augmentation: Cognitive augmentation is the closest we currently have to true artificial intelligence. Cognitive computers, such as IBM's Watson, are able to handle unstructured data and provide answers to complex queries, enabling them to complete tasks that could once only be performed by humans.

Though these categories denote levels of complexity, it is better not to think of automation technologies as stages through which an organization must progress. Instead, each technology is best suited to particular types of work and may be used in concert to achieve larger goals.

Intelligent automation (IA) is a term increasingly applied to this concept of combining multiple automation technologies to solve complex business issues. For example, organizations are looking to use RPA with machine learning, NLP and digital character recognition to help address regulatory compliance challenges and process high-volume, low-complexity insurance claims.

Jobs changing, not necessarily replaced

Doomsday predictions about automation's impacts to the workforce have been in the headlines for the past few years, with total job loss a significant concern. For example, in 2014 Gartner research director Peter Sondergaard stated, "Gartner predicts one in three jobs will be converted to software, robots and smart machines by 2025." Yet while there are pockets of extensive automation within the industry, generous estimates cannot put the average rate of automation above 5 percent — significantly behind the rate required to achieve replacement of a full third of the workforce in 7 years.

While initial predictions were for automation to result in wholesale replacement of human workers, that is not what we are seeing play out in immediate timeframes. Instead, these technologies are being used to enhance or support the work of human employees. Automation capabilities can help remove the burden of repetitive administrative work or provide information to help individuals make better decisions, allowing employees to focus on

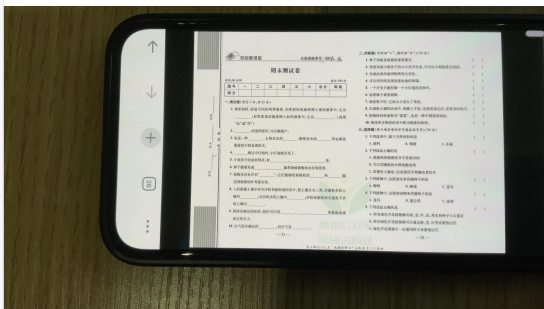
Intelligent automation

(IA) is a term increasingly applied to this concept of combining multiple automation technologies to solve complex business issues.

Today's organizational challenges



Image



PaddleOCR-VL-1.5

夺冠新课堂 三年级科学下·DX

期末测试卷

时间:60分钟 满分:100分

题号	一	二	三	四	五	六	总分	等级
得分								

一、填空题(每空1分,共23分)

1. 体积相同,质量不同的两种液体,如果把轻的液体倒入重的液体中,它会___;如果把重的液体倒入轻的液体中,它会___。(选填“沉”或“浮”)
2. ___的透明度好,可以做窗户
3. 电是一种___,太阳发出的___、物体发出的___等都是能量的不同表现形式。
4. ___透过小灯泡时,小灯泡就发光了。
5. 小狗房子的选材要求:要___、___、___等。
6. 种子能萌发成___能帮助植物吸收水分和营养。
7. 植物茎内有许多“___”,它们能够把根吸收的___和___输送到植物的叶等器官。
8. 人们根据土壤中所含沙粒和黏粒量的多少,把土壤分为三类:含黏粒多的土壤叫___,含沙粒多的土壤叫___,沙粒和黏粒的含量差不多的土壤叫___。
9. 固体有确定的形状,我们可以用___、___等数值来描述它的大小。
10. 空气没有确定的___,但空气有___。

二、判断题(对的画“√”,错的画“×”)(10分)

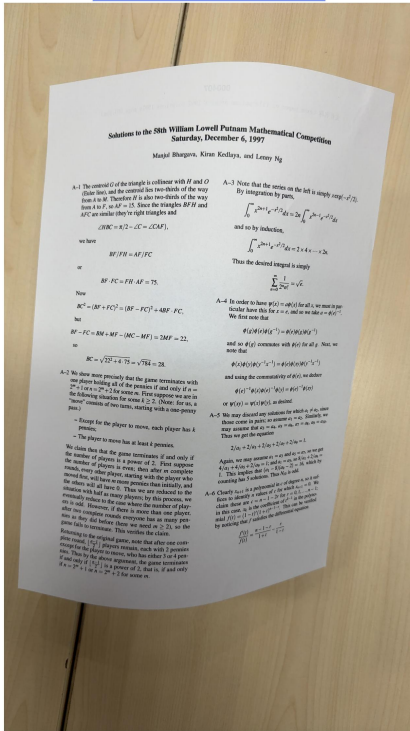
1. 种子和根是植物的重要器官。 ()
2. 要想知道小狗房子的大小是否合适,可以让小狗钻进去试试。 ()

3. 变成油条的面团物质发生变化。 ()
4. 可以用导线直接连接电池的两端。 ()
5. 一个开关只能控制一个小灯泡的亮和灭。 ()
6. 油菜属于蔬菜植物。 ()
7. 清洗梨子时,它的大小发生了变化。 ()
8. 在观察土壤的活动中,要戴上手套,完成活动之后,还要及时洗手。 ()
9. 把物体的质量称为“重量”,这是一种不规范的讲法。 ()
10. 物体所含物质的多少称为物体的体积。 ()

三、选择题(将正确答案的序号填在括号里) (24分)

1. 下列选项中,属于天然材料的是 ()
A. 塑料 B. 钢筋 C. 木板 D. 纸
2. 下列说法正确的是 ()
A. 绝缘体的绝缘性并不是绝对的
B. 可以用潮湿的木棒接触电线
C. 发现有人触电,应直接用手将触电者拉开
D. 下列植物中,会借助水来传播种子的是 ()
A. 柳树 B. 睡莲 C. 苍耳
D. 蒲公英
3. 下列植物中,会借助动物来传播种子的是 ()
A. 苍耳 B. 蒲公英 C. 油菜
D. 柳树
4. 下列说法正确的是 ()
A. 所有绿色开花植物都有根、茎、叶、花、果实和种子六大器官
B. 所有绿色开花植物都可以通过根、茎、叶等来繁殖后代
C. 绿色开花植物不一定都用种子来繁殖后代

Figure A3 | The Markdown Output for Screen Photography.



Solutions to the 58th William Lowell Putnam Mathematical Competition Saturday, December 6, 1997

Manjul Bhargava, Kiran Kedlaya, and Lenny Ng

A-1 The centroid G of the triangle is collinear with H and O (Euler line), and the centroid lies two-thirds of the way from A to O . Therefore H is also two-thirds of the way from A to O . Since the triangles BHF and AFC are similar (they're right triangles and

$$\angle HBC = \pi/2 - \angle C = \angle CAF,$$

we have

$$BF/FH = AF/FC$$

or

$$BF \cdot FC = FH \cdot AF = 75.$$

Now

$$BC^2 = (BF + FC)^2 = (BF - FC)^2 + 4BF \cdot FC,$$

but

$$BF - FC = BM + MP - (MC - MP) = 2MP = 22,$$

so

$$BC = \sqrt{22^2 + 4 \cdot 75} = \sqrt{784} = 28$$

A-2 We show more precisely that the game terminates with one player holding all of the pennies if and only if $n = 2^m + 1$ or $n = 2^m + 2$ for some m . First suppose we are in the following situation for some $k \geq 2$. (Note: for us, a "move" consists of two turns, starting with a one-penny pass.)

- Except for the player to move, each player has k pennies;
- The player to move has at least k pennies.

We claim then that the game terminates if and only if the number of players is a power of 2. First suppose rounds, every other player, starting with the player who moved first, will have m more pennies than initially, and the others will all have 0. Thus we are reduced to the situation with half as many players. By this process, we eventually reduce to the case where the number of players is odd. However, if there is more than one player, after two complete rounds everyone has as many pennies as they did before (here we need $m \geq 2$), so the game fails to terminate. This verifies the claim. Returning to the original game, note that after one complete round, $\lfloor \frac{n-1}{2} \rfloor$ players remain, each with 2 pennies except for the player to move, who has either 3 or 4 pennies. Thus by the above argument, the game terminates if and only if $\lfloor \frac{n-1}{2} \rfloor$ is a power of 2, that is, if and only if $n = 2^m + 1$ or $n = 2^m + 2$ for some m .

A-3 Note that the series on the left is simply $x \exp(-x^2/2)$. By integration by parts,

$$\int_0^{\infty} x^{2n+1} e^{-x^2/2} dx = 2n \int_0^{\infty} x^{2n-1} e^{-x^2/2} dx$$

and so by induction,

$$\int_0^{\infty} x^{2n+1} e^{-x^2/2} dx = 2 \times 4 \times \dots \times 2n.$$

Thus the desired integral is simply

$$\sum_{n=0}^{\infty} \frac{1}{2^n n!} = \sqrt{e}.$$

A-4 In order to have $\psi(x) = a\phi(x)$ for all x , we must in particular have this for $x = 0$, and so we take $a = \phi(0)^{-1}$. We first note that

$$\phi(g)\phi(e)\phi(g^{-1}) = \phi(e)\phi(g)\phi(g^{-1})$$

and so $\phi(g)$ commutes with $\phi(e)$ for all g . Next, we note that

$$\phi(x)\phi(y)\phi(y^{-1}x^{-1}) = \phi(e)\phi(xy)\phi(y^{-1}x^{-1})$$

and using the commutativity of $\phi(e)$, we deduce

$$\phi(x)^{-1}\phi(x)\phi(e)^{-1}\phi(y) = \phi(e)^{-1}\phi(xy)$$

or $\psi(xy) = \psi(x)\psi(y)$, as desired.

A-5 We may discard any solutions for which $a_1 \neq a_2$, since those come in pairs; so assume $a_1 = a_2$. Similarly, we may assume that $a_3 = a_4$, $a_5 = a_6$, $a_7 = a_8$, $a_9 = a_{10}$. Thus we get the equation

$$2/a_1 + 2/a_3 + 2/a_5 + 2/a_7 + 2/a_9 = 1.$$

Again, we may assume $a_1 = a_3$ and $a_5 = a_7$, so we get $4/a_1 + 4/a_5 + 2/a_9 = 1$; and $a_1 = a_5$, so $8/a_1 + 2/a_9 = 1$. This implies that $(a_1 - 8)(a_9 - 2) = 16$, which by counting has 5 solutions. Thus N_5 is odd.

A-6 Clearly x_{n+1} is a polynomial in c of degree n , so it suffices to identify n values of c for which $x_{n+1} = 0$. We claim these are $c = n-1, 2, \dots, n-1$; in this case, x_n is the coefficient of t^{n-1} in the polynomial $f(t) = (1-t)^n(1+t)^{n-1}$. This can be verified by noticing that f satisfies the differential equation

$$\frac{f'(t)}{f(t)} = \frac{n-1-t}{1+t} - \frac{r}{1-t}$$



[PDF] No Safe Place



There's nothing more dangerous than a familiar face... As funeral mourners stand in silence at Ragmulin cemetery, a deafening cry cuts through the air. Lying crumpled at the bottom of an open grave is the bloodied body of a young woman, and Detective Lottie Parker is called in to investigate... Read More...

[PDF] Portrait of an Unknown Woman



In a spellbinding new masterpiece by #1 New York Times bestselling author Daniel Silva, Gabriel Allan undertakes a high-stakes search for the greatest art forger who ever lived. Legendary spy and art restorer Gabriel Allan has at long last severed ties with Israeli intelligence and settled quietly in... Read More...

[PDF] The 6:20 Man



A cryptic murder pulls a former soldier turned financial analyst deep into the corruption and menace that prowls beneath the opulent world of finance, in this #1 New York Times bestselling thriller from David Baldacci. Every day without fail, Travis Devine puts on a cheap suit, grabs his faux-leather... Read More...

[PDF] It Ends with Us



In this "brave and heartbreaking novel that digs its claws into you and doesn't let go, long after you've finished it" (Anna Todd, New York Times bestselling author of All Your Perfects), a workaholic with a too-good-to-be-true romance can't stop thinking... Read More...

[PDF] Thunder Bay



Storm Island's secrets are worth killing for in this immersive, unrelenting thriller for readers of All the Missing Girls and Neon Prep —this crime novel has it all! (Publishers Weekly, starred review). When reporter Rebecca Connolly gets a tip that suspected murderer Roddie Drummond... Read More...

Figure A5 | The Markdown Output for Warping.

E.2. Layout Analysis

E.2.1. Layout Analysis for Real-world Documents



Figure A6 | Comparison of Layout Analysis Results between PaddleOCR-VL and PaddleOCR-VL-1.5 for Warping.

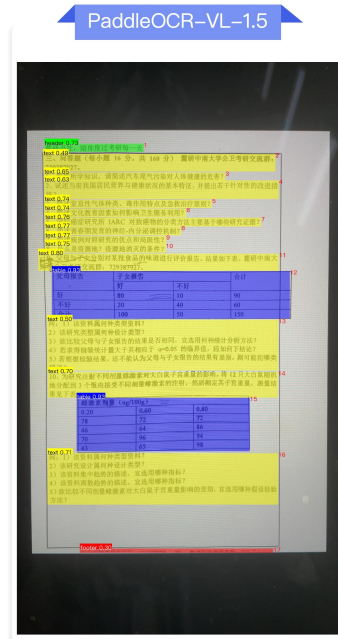
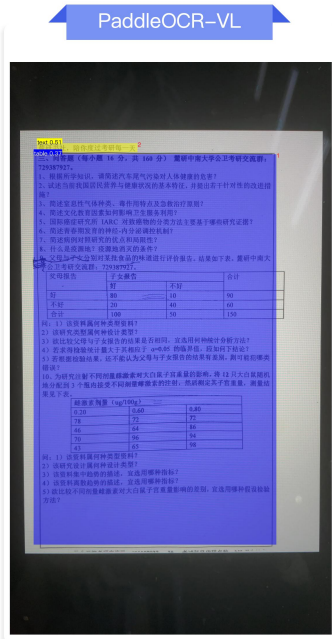
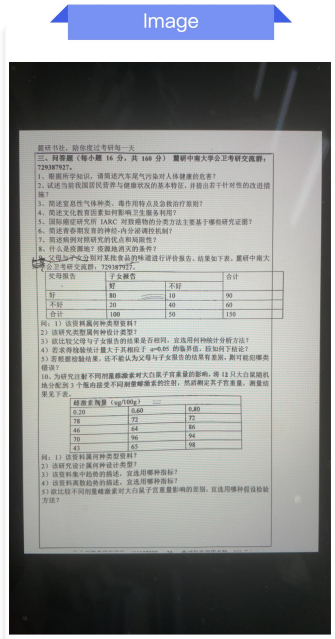
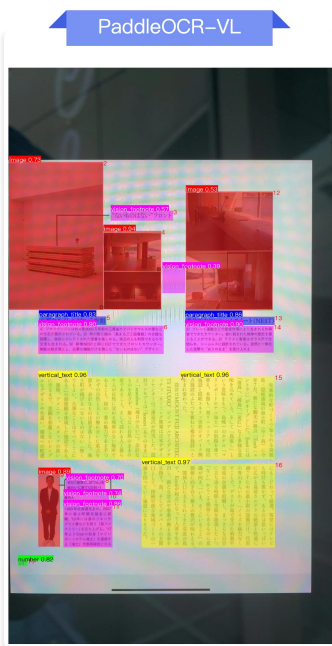
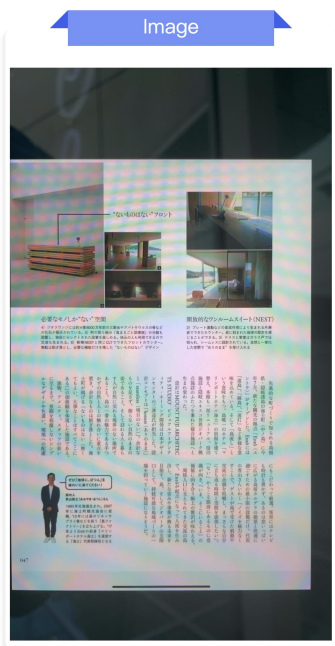


Figure A7 | Comparison of Layout Analysis Results between PaddleOCR-VL and PaddleOCR-VL-1.5 for Screen Photography.



Figure A8 | Comparison of Layout Analysis Results between PaddleOCR-VL and PaddleOCR-VL-1.5 for Skew.

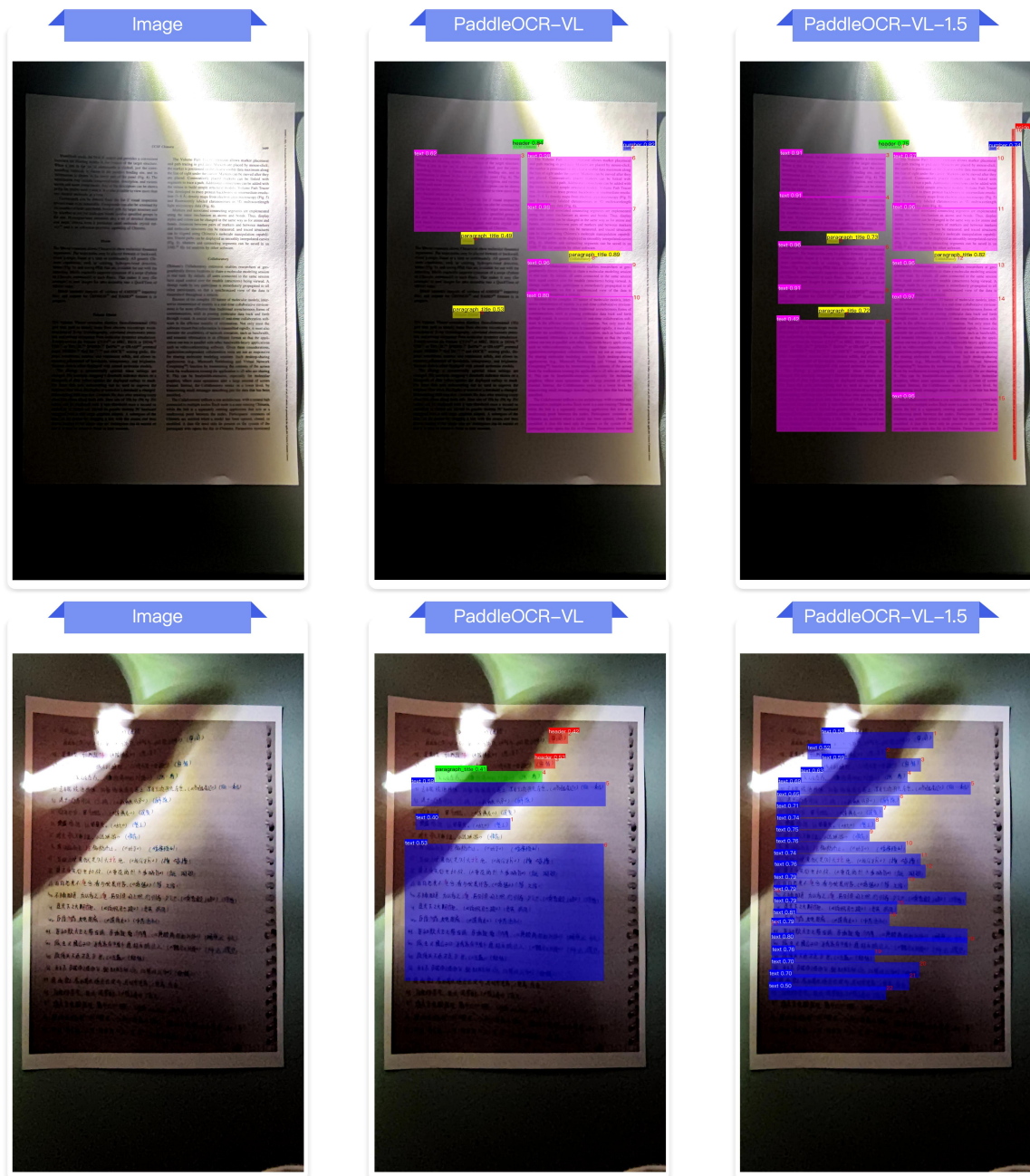


Figure A9 | Comparison of Layout Analysis Results between PaddleOCR-VL and PaddleOCR-VL-1.5 for Illumination.

E.2.2. Layout Analysis for New Scenarios

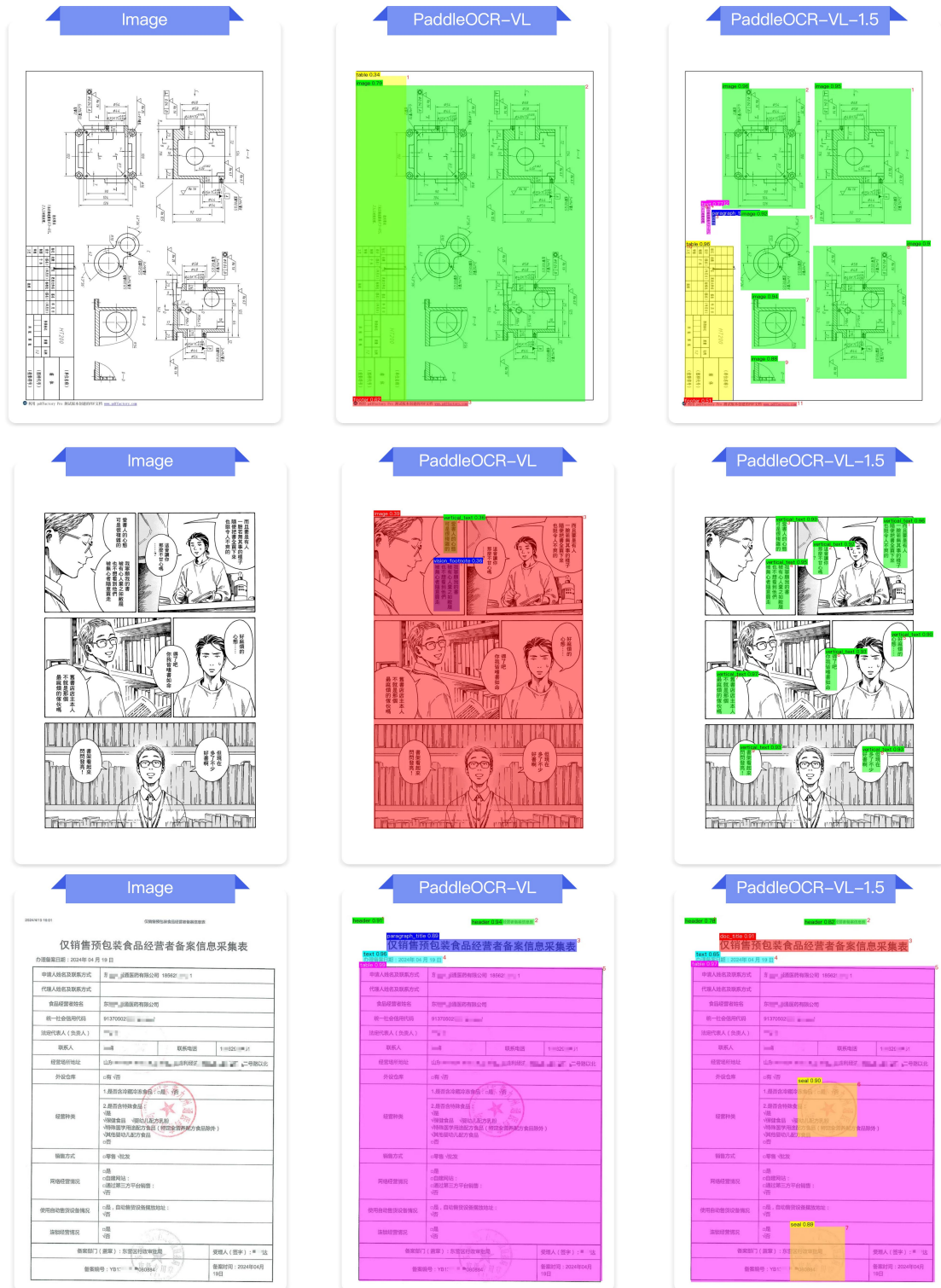


Figure A10 | Comparison of Layout Analysis Results between PaddleOCR-VL and PaddleOCR-VL-1.5 for New Scenarios.

E.3. Text Recognition

E.3.1. Text Recognition for Text decoration

<p>Image</p> <p>【题目】仿照画线句子，在横线处写上两个语意连贯的句子。</p> <p>爱读书，是一种美德。世界上有大成就的人，对人类有特殊贡献的人，几乎都是爱读书的人。读书，使人思维活跃，聪颖智慧；_____；_____。</p>	<p>PaddleOCR-VL</p> <p>【题目】仿照画线句子，在横线处写上两个语意连贯的句子。</p> <p>爱读书，是一种美德。世界上有大成就的人，对人类有特殊贡献的人，几乎都是爱读书的人。读书，使人思维活跃，聪颖智慧；_____；_____。</p> <p>Underlines Lost</p>	<p>PaddleOCR-VL-1.5</p> <p>【题目】仿照画线句子，在横线处写上两个语意连贯的句子。</p> <p>爱读书，是一种美德。世界上有大成就的人，对人类有特殊贡献的人，几乎都是爱读书的人。读书，使人思维活跃，聪颖智慧；_____；_____。</p>
<p>Image</p> <p>一、下列词语中加点字的注音全都正确的一项是()</p> <p>A. 舀水(yǎo) 校对(xiào) B. 草率(shuài) 抹杀(mǒ) C. 洗濯(zǎo) 调羹(diào) D. 轻捷(xié) 绞肉(jiǎo)</p>	<p>PaddleOCR-VL</p> <p>一、下列词语中加点字的注音全都正确的一项是()</p> <p>A. 舀水(yǎo) 校对(xiào) B. 草率(shuài) 抹杀(mǒ) C. 洗濯(zǎo) 调羹(diào) D. 轻捷(xié) 绞肉(jiǎo)</p> <p>Emphasis Mark Lost</p>	<p>PaddleOCR-VL-1.5</p> <p>一、下列词语中加点字的注音全都正确的一项是()</p> <p>A. 舀水(yǎo) 校对(xiào) B. 草率(shuài) 抹杀(mǒ) C. 洗濯(zào) 调羹(diào) D. 轻捷(xié) 绞肉(jiǎo)</p>
<p>Image</p> <p>判断句子中画线部分发音是否相同，相同的写“T”，不同的写“F”。(4分)</p> <p>() 1. My grandpa is happy to see the green grass. () 2. There is a brown umbrella in the library. () 3. My brother brings me a black crayon. I like it. () 4. My grey dog has some bread for breakfast.</p>	<p>PaddleOCR-VL</p> <p>一判断句子中画线部分发音是否相同，相同的写“T”，不同的写“F”。(4分)</p> <p>() 1. My grandpa is happy to see the green grass. () 2. There is a brown umbrella in the library. () 3. My brother brings me a black crayon. I like it. () 4. My grey dog has some bread for breakfast.</p> <p>Underlines Lost</p>	<p>PaddleOCR-VL-1.5</p> <p>判断句子中画线部分发音是否相同，相同的写“T”，不同的写“F”。(4分)</p> <p>() 1. My grandpa is happy to see the green grass. () 2. There is a brown umbrella in the library. () 3. My brother brings me a black crayon. I like it. () 4. My grey dog has some bread for breakfast.</p>
<p>Image</p> <p>阅读课内片段，完成练习。</p> <p>老天不负苦心人，他的儿子考取了。送我去入学的时候，依旧是那只小船，依旧是姑爹和父亲轮换划船，不过父亲不划船的时候，便抓紧时间为我缝补棉裤，因我那长期卧床的母亲未能给我备齐行装。我从舱里往外看，父亲那弯腰低头缝补的背影挡住了我的视线。后来我读到朱自清先生的《背影》时，这个船舱里的背影也就分外明显，永生难忘！</p> <p>不仅是背影时在我眼前显现，鲁迅笔底的乌篷船也永远是那么亲切。虽然姑爹小船上盖的只是破旧的篷，远比不上绍兴的乌篷船精致，但姑爹的小渔船仍然是那么亲切，那么难忘……我什么时候能够用自己手中的笔，把那只载着父爱的小船画出来就好了！</p> <p>1. “老天不负苦心人”的意思是_____。“苦心人”在本段文字中指_____。</p> <p>2. 素养练·体会感情 本段文字描绘的场面可以用_____四个字概括，文中写到朱自清先生的《背影》和乌篷船的作用是_____。</p> <p>3. 从选文中画波浪线的句子中可以体会到()</p> <p>A. 作者对父亲深深的怀念和感激之情。 B. 这只小船对作者来说非常熟悉。 C. 作者坐这只小船的次数最多，很怀念小船。</p>	<p>PaddleOCR-VL</p> <p>阅读课内片段，完成练习。</p> <p>老天不负苦心人，他的儿子考取了。送我去入学的时候，依旧是那只小船，依旧是姑爹和父亲轮换划船，不过父亲不划船的时候，便抓紧时间为我缝补棉裤，因我那长期卧床的母亲未能给我备齐行装。我从舱里往外看，父亲那弯腰低头缝补的背影挡住了我的视线。后来我读到朱自清先生的《背影》时，这个船舱里的背影也就分外明显，永生难忘！</p> <p>不仅是背影时在我眼前显现，鲁迅笔底的乌篷船也永远是那么亲切。虽然姑爹小船上盖的只是破旧的篷，远比不上绍兴的乌篷船精致，但姑爹的小渔船仍然是那么亲切，那么难忘……我什么时候能够用自己手中的笔，把那只载着父爱的小船画出来就好了！</p> <p>1. “老天不负苦心人”的意思是_____。“苦心人”在本段文字中指_____。</p> <p>2. 素养练·体会感情 本段文字描绘的场面可以用_____四个字概括，文中写到朱自清先生的《背影》和乌篷船的作用是_____。</p> <p>3. 从选文中画波浪线的句子中可以体会到()</p> <p>A. 作者对父亲深深的怀念和感激之情。 B. 这只小船对作者来说非常熟悉。 C. 作者坐这只小船的次数最多，很怀念小船。</p> <p>Wave Underlines Lost</p>	<p>PaddleOCR-VL-1.5</p> <p>阅读课内片段，完成练习。</p> <p>老天不负苦心人，他的儿子考取了。送我去入学的时候，依旧是那只小船，依旧是姑爹和父亲轮换划船，不过父亲不划船的时候，便抓紧时间为我缝补棉裤，因我那长期卧床的母亲未能给我备齐行装。我从舱里往外看，父亲那弯腰低头缝补的背影挡住了我的视线。后来我读到朱自清先生的《背影》时，这个船舱里的背影也就分外明显，永生难忘！</p> <p>不仅是背影时在我眼前显现，鲁迅笔底的乌篷船也永远是那么亲切。虽然姑爹小船上盖的只是破旧的篷，远比不上绍兴的乌篷船精致，但姑爹的小渔船仍然是那么亲切，那么难忘……我什么时候能够用自己手中的笔，把那只载着父爱的小船画出来就好了！</p> <p>1. “老天不负苦心人”的意思是_____。“苦心人”在本段文字中指_____。</p> <p>2. 素养练·体会感情 本段文字描绘的场面可以用_____四个字概括，文中写到朱自清先生的《背影》和乌篷船的作用是_____。</p> <p>3. 从选文中画波浪线的句子中可以体会到()</p> <p>A. 作者对父亲深深的怀念和感激之情。 B. 这只小船对作者来说非常熟悉。 C. 作者坐这只小船的次数最多，很怀念小船。</p>

Figure A11 | Markdown Output Comparison between PaddleOCR-VL and PaddleOCR-VL-1.5 on Text Decoration Documents.

E.3.2. Text Recognition for Special characters

Image	PaddleOCR-VL	PaddleOCR-VL-1.5
<p>点拨：朗读时需注意“之、初、善、专”都是翘舌音。人/之初△，性/本善△，性/相近△，习/相远△。苟/不教△，性/乃迂△，教/之道△，贵/以专△。子/不学△，非/所宜△。幼/不学△老/何为？玉/不琢△，不/成器△。人/不学△，不/知义△。在背诵课文前，我们首先要理解课文内容并熟读，可以拍手读，也可以同桌对读，用多种形式达到熟读成诵。其次，掌握课文的结构特点。本文共四句话，每句话的构句方式都相同。第一小节每行的尾字都押韵；第二小节的一、三、四行尾字押韵，而且每行的前半句都是“x不x”的构句形式。了解这些特点后，我们就很容易背诵了。</p>	<p>点拨：朗读时需注意“之、初、善、专”都是翘舌音。人/之初△，性/本善△，性/相近△，习/相远△。苟/不教△，性/乃迂△，教/之道△，贵/以专△。子/不学△，非/所宜△。幼/不学△老/何为？玉/不琢△，不/成器△。人/不学△，不/知义△。在背诵课文前，我们首先要理解课文内容并熟读，可以拍手读，也可以同桌对读，用多种形式达到熟读成诵。其次，掌握课文的结构特点。本文共四句话，每句话的构句方式都相同。第一小节每行的尾字都押韵；第二小节的一、三、四行尾字押韵，而且每行的前半句都是“x不x”的构句形式。了解这些特点后，我们就很容易背诵了。</p> <p>Special Character Recognition Error</p>	<p>点拨：朗读时需注意“之、初、善、专”都是翘舌音。人/之初△，性/本善△，性/相近△，习/相远△。苟/不教△，性/乃迂△，教/之道△，贵/以专△。子/不学△，非/所宜△。幼/不学△老/何为？玉/不琢△，不/成器△。人/不学△，不/知义△。在背诵课文前，我们首先要理解课文内容并熟读，可以拍手读，也可以同桌对读，用多种形式达到熟读成诵。其次，掌握课文的结构特点。本文共四句话，每句话的构句方式都相同。第一小节每行的尾字都押韵；第二小节的一、三、四行尾字押韵，而且每行的前半句都是“x不x”的构句形式。了解这些特点后，我们就很容易背诵了。</p>
<p>3. 设 N_A 为阿伏加德罗常数的值。下列叙述正确的是</p> <p>A. 1 L 0.1 mol·L⁻¹ NaClO 溶液中含 ClO⁻ 数目为 0.1 N_A</p> <p>B. 1 mol NaCl 固体中，含离子数为 2 N_A</p> <p>C. 标准状况下，22.4 L 氧气、氮气和 CO 的混合气体中含有 2 N_A 个分子</p> <p>D. 将 Cl₂ 与 NaOH 溶液反应制备消毒液，消耗 1 mol Cl₂ 转移电子数为 2 N_A</p>	<p>3. 设 N_A 为阿伏加德罗常数的值。下列叙述正确的是</p> <p>A. 1 L 0.1 mol·L⁻¹ NaClO 溶液中含 ClO⁻ 数目为 0.1 N_A</p> <p>B. 1 mol NaCl 固体中，含离子数为 2 N_A</p> <p>C. 标准状况下，22.4 L 氧气、氮气和 CO 的混合气体中含有 2 N_A 个分子</p> <p>D. 将 Cl₂ 与 NaOH 溶液反应制备消毒液，消耗 1 mol Cl₂ 转移电子数为 2 N_A</p> <p>Special Character Lost</p>	<p>3. 设 N_A 为阿伏加德罗常数的值。下列叙述正确的是</p> <p>A. 1 L 0.1 mol·L⁻¹ NaClO 溶液中含 ClO⁻ 数目为 0.1 N_A</p> <p>B. 1 mol NaCl 固体中，含离子数为 2 N_A</p> <p>C. 标准状况下，22.4 L 氧气、氮气和 CO 的混合气体中含有 2 N_A 个分子</p> <p>D. 将 Cl₂ 与 NaOH 溶液反应制备消毒液，消耗 1 mol Cl₂ 转移电子数为 2 N_A</p>
<p>箭头符号</p> <ul style="list-style-type: none"> • ↑ ↓ ← → • ↖ ↗ ↘ ↙ • ↔ • ⇌ <p>数学符号</p> <ul style="list-style-type: none"> • ∑ ∏ ∫ ∂ • ± √ ∞ ≈ • ≠ ≤ ≥ ≡ <p>货币符号</p> <ul style="list-style-type: none"> • \$ € £ ¥ • ₩ ₹ 	<p>箭头符号</p> <ul style="list-style-type: none"> • ↑ ↓ ← → • ↖ ↗ ↘ ↙ • ↔ • ⇌ <p>数学符号</p> <ul style="list-style-type: none"> • ∑ ∏ ∫ ∂ • ± √ ∞ ≈ • ≠ ≤ ≥ ≡ <p>货币符号</p> <ul style="list-style-type: none"> • \$ € £ ¥ <p>Special Character Recognition Error</p> <p>Special Character Lost</p>	<p>箭头符号</p> <ul style="list-style-type: none"> • ↑ ↓ ← → • ↖ ↗ ↘ ↙ • ↔ • ⇌ <p>数学符号</p> <ul style="list-style-type: none"> • ∑ ∏ ∫ ∂ • ± √ ∞ ≈ • ≠ ≤ ≥ ≡ <p>货币符号</p> <ul style="list-style-type: none"> • \$ € £ ¥ • ₩ ₹

Figure A12 | Markdown Output Comparison between PaddleOCR-VL and PaddleOCR-VL-1.5 on Special Characters Documents.

E.4. Table Recognition

E.4.1. Table Recognition for General Tables

Image									
阶段	同意	需修改	不同意	修改意见	预测因素	同意	需修改	不同意	修改意见
入职					认知加工				
					神经质人格				
					心理痛苦				
术前					认知加工				
					应对方式				
					社会支持				
术后					自我披露				
					心理痛苦				
					躯体感觉运动障碍				
出院前				日常生活能力					
					功能恢复				

PaddleOCR-VL									
阶段	同意	需修改	不同意	修改意见	预测因素	同意	需修改	不同意	修改意见
入职					认知加工				
					神经质人格				
					心理痛苦				
术前					认知加工				
					应对方式				
					社会支持				
术后					自我披露				
					心理痛苦				
					躯体感觉运动障碍				
出院前				日常生活能力					
					功能恢复				

PaddleOCR-VL-1.5									
阶段	同意	需修改	不同意	修改意见	预测因素	同意	需修改	不同意	修改意见
入职					认知加工				
					神经质人格				
					心理痛苦				
术前					认知加工				
					应对方式				
					社会支持				
术后					自我披露				
					心理痛苦				
					躯体感觉运动障碍				
出院前				日常生活能力					
					功能恢复				

Image			
名称	直线	射线	线段
图形			
表示	直线AB或直线l	射线AB或射线l	线段AB或线段l
基本事实	两点确定一条直线	—	两点之间，线段最短

PaddleOCR-VL			
名称	直线	射线	线段
图形	ABI	ABI	
表示	直线AB或直线l	射线AB或射线l	线段AB或线段l
基本事实	两点确定一条直线	—	两点之间，线段最短

PaddleOCR-VL-1.5			
名称	直线	射线	线段
图形			
表示	直线AB或直线l	射线AB或射线l	线段AB或线段l
基本事实	两点确定一条直线	—	两点之间，线段最短

Image		
已知、解法	已知条件	解法步骤
三角形模型 	两直角边 (如 a, b)	由 $\tan A = \frac{a}{b}$, 求 $\angle A, \angle B = 90^\circ - \angle A, c = \sqrt{a^2 + b^2}$
	斜边、一直角边 (如 c, a)	由 $\sin A = \frac{a}{c}$, 求 $\angle A, \angle B = 90^\circ - \angle A, b = \sqrt{c^2 - a^2}$
	一直角边和一角 (如 $\angle A, b$)	锐角、邻边 $\angle B = 90^\circ - \angle A, a = b \cdot \tan A, c = \frac{b}{\cos A}$
	一边一角 (如 $\angle A, a$)	锐角、对边 $\angle B = 90^\circ - \angle A, b = \frac{a}{\tan A}, c = \frac{a}{\sin A}$
	斜边、锐角 (如 c, $\angle A$)	$\angle B = 90^\circ - \angle A, a = c \sin A, b = c \cos A$

PaddleOCR-VL		
已知、解法三角形模型	已知条件	解法步骤
	两直角边 (如 a, b)	由 $\tan A = \frac{a}{b}$, 求 $\angle A, \angle B = 90^\circ - \angle A, c = \sqrt{a^2 + b^2}$
	斜边、一直角边 (如 c, a)	由 $\sin A = \frac{a}{c}$, 求 $\angle A, \angle B = 90^\circ - \angle A, b = \sqrt{c^2 - a^2}$
	一直角边和一角 (如 $\angle A, b$)	锐角、邻边 $\angle B = 90^\circ - \angle A, a = b \cdot \tan A, c = \frac{b}{\cos A}$
	一边一角 (如 $\angle A, a$)	锐角、对边 $\angle B = 90^\circ - \angle A, b = \frac{a}{\tan A}, c = \frac{a}{\sin A}$
	斜边、锐角 (如 c, $\angle A$)	$\angle B = 90^\circ - \angle A, a = c \sin A, b = c \cos A$

PaddleOCR-VL-1.5		
已知、解法三角形模型	已知条件	解法步骤
	两直角边 (如 a, b)	由 $\tan A = \frac{a}{b}$, 求 $\angle A, \angle B = 90^\circ - \angle A, c = \sqrt{a^2 + b^2}$
	斜边、一直角边 (如 c, a)	由 $\sin A = \frac{a}{c}$, 求 $\angle A, \angle B = 90^\circ - \angle A, b = \sqrt{c^2 - a^2}$
	一直角边和一角 (如 $\angle A, b$)	锐角、邻边 $\angle B = 90^\circ - \angle A, a = b \cdot \tan A, c = \frac{b}{\cos A}$
	一边一角 (如 $\angle A, a$)	锐角、对边 $\angle B = 90^\circ - \angle A, b = \frac{a}{\tan A}, c = \frac{a}{\sin A}$
	斜边、锐角 (如 c, $\angle A$)	$\angle B = 90^\circ - \angle A, a = c \sin A, b = c \cos A$

Figure A14 | Markdown Output Comparison between PaddleOCR-VL and PaddleOCR-VL-1.5 on General Tables.

E.4.2. Table Recognition for Multiple Languages



Figure A15 | Markdown Output Comparison between PaddleOCR-VL and PaddleOCR-VL-1.5 on Multilingual Tables.

E.4.3. Table Recognition for Cross-Page Tables

Image

PaddleOCR-VL

PaddleOCR-VL-1.5

Image

PaddleOCR-VL

PaddleOCR-VL-1.5

Figure A16 | Markdown Output Comparison between PaddleOCR-VL and PaddleOCR-VL-1.5 on Cross-Page Tables.

E.5. Formula Recognition

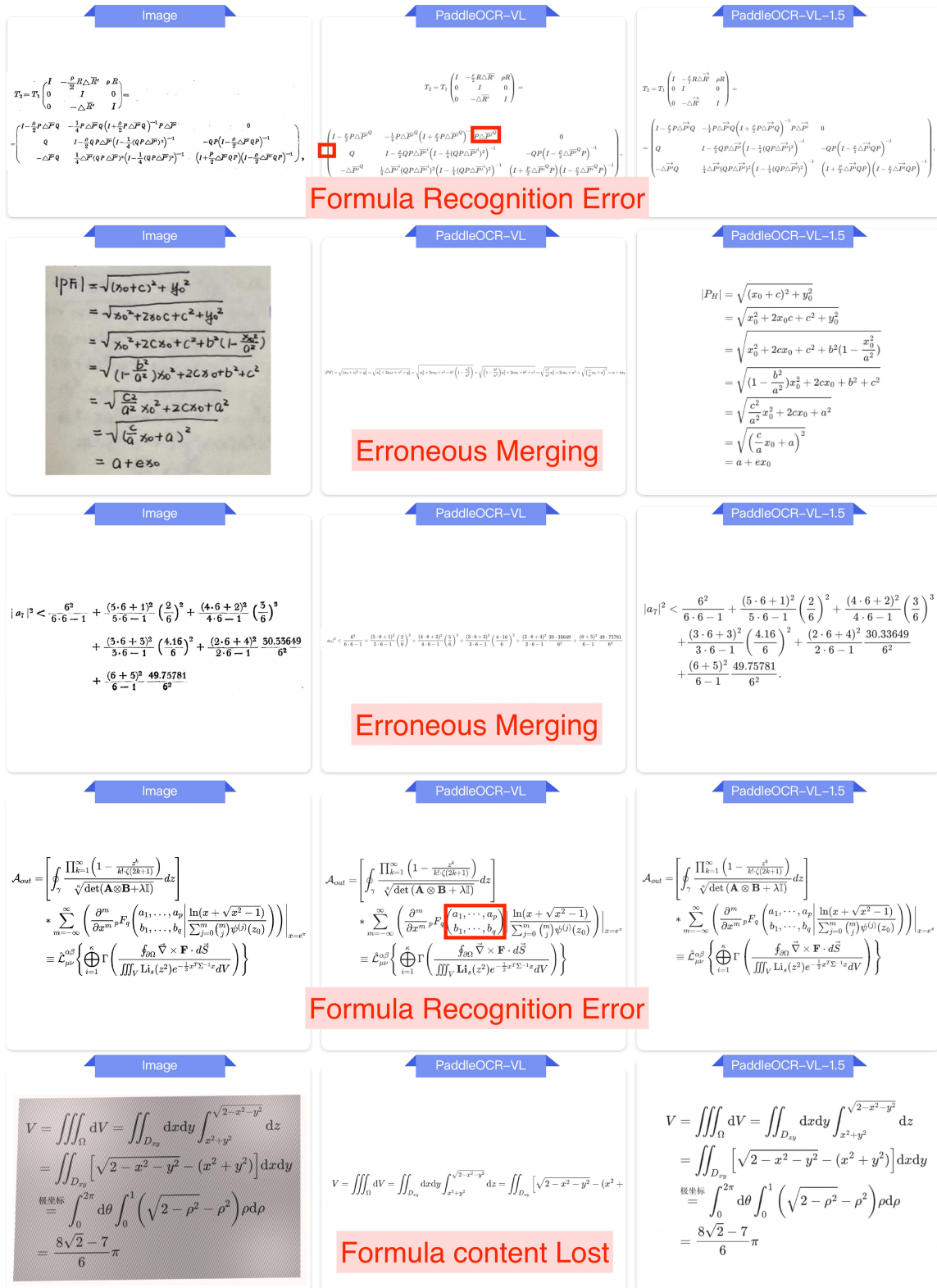


Figure A17 | Markdown Output Comparison between PaddleOCR-VL and PaddleOCR-VL-1.5 on various types of Formulas.

E.6. Seal Recognition

<p style="text-align: center;">Image</p> 	<p style="text-align: center;">PaddleOCR-VL-1.5</p> <p>浙江省台州医院 医疗业务专用章 (一) 3310821031712</p>
<p style="text-align: center;">Image</p> 	<p style="text-align: center;">PaddleOCR-VL-1.5</p> <p>烟台盈泰企业管理咨询有限公司 3706023098276</p>
<p style="text-align: center;">Image</p> 	<p style="text-align: center;">PaddleOCR-VL-1.5</p> <p>德阳九鼎电气有限公司 检验专用章</p>
<p style="text-align: center;">Image</p> 	<p style="text-align: center;">PaddleOCR-VL-1.5</p> <p>全国统一发票监制章 国家税务总局 宁波市税务局</p>

Figure A18 | The markdown output for various types of Seals 1.



Figure A19 | The markdown output for various types of Seals 2.

<p>Image</p> 	<p>PaddleOCR-VL-1.5</p> <p>天津市招生委员会 办公室 录取专用章</p>
<p>Image</p> 	<p>PaddleOCR-VL-1.5</p> <p>北京大学 招生办公室</p>
<p>Image</p> 	<p>PaddleOCR-VL-1.5</p> <p>Christmas 2023 St. Dunstan's Church Canterbury 2.11.23</p>
<p>Image</p> 	<p>PaddleOCR-VL-1.5</p> <p>100 YEARS OF PHILATELY IN HASTINGS ROBERTSON ST 2 NOV 2023 1923 - 2023</p>

Figure A20 | The markdown output for various types of Seals 3.

E.7. Text Spotting



Figure A21 | Text spotting results on various types of documents.